Fabrication of Amorphous Microstructure for Distortion Free Structural Color

Mohammad Harun-ur-Rashid

Fabrication of Amorphous Microstructure for Distortion Free Structural Color

A thesis submitted to the Department of Molecular Design & Engineering
in conformity with the requirements for
the degree of Doctor of Engineering

Submitted By

Mohammad Harun-ur-Rashid
Student ID#480766045
Molecular Assembly System Laboratory
Department of Molecular Design & Engineering
Graduate School of Engineering
Nagoya University
Nagoya, Japan
March, 2010

TO

MY BELOVED PARENTS

Acknowledgements

This thesis arose in part out of years of research that has been done since I came to Prof. Dr. Seki's group. By that time, I have worked with a great number of people whose contribution in assorted ways to the research and the making of the thesis deserved special mention. It is a pleasure to convey my gratitude to them all in my humble acknowledgment.

In the first place I would like to take this opportunity with great pleasure to record my gratitude to **Prof. Dr. Y. Takeoka**, my academic supervisor, for his supervision, advice, and guidance from the very early stage of this research as well as giving me extraordinary experiences throughout the work. Above all and the most needed, he provided me unflinching encouragement and support in various ways. His truly scientist intuition has made him as a constant oasis of ideas and passions in science, which exceptionally inspire and enrich my growth as a student, a researcher and a scientist want to be. I gratefully acknowledge for his advice, supervision, and crucial contribution, which made him a backbone of this research and so to this thesis. He has made available his support in a number of ways. I am indebted to him more than he knows. I feel myself an extraordinarily fortunate in having **Prof. Dr. Y. Takeoka** as my supervisor. Thank you.

Many thanks go in particular to **Prof. Dr. T. Seki** and **Prof. Dr. S. Nagano**. I am much indebted to Prof. Dr. T. Seki for his valuable advice in science discussion, overall supervision and furthermore, his critical comments about my research work. I have also benefited by advice and guidance from Prof. Dr. S. Nagano, who also always kindly grants me his time even for answering some of my unintelligent questions about different scientific terms. I convey my special acknowledge to **Mr. M. Ishii** and **H. Nakamura** of Toyota Central R&D Laboratories, Inc., Aichi, Japan, for their indispensable support to this research.

I am also greatly indebted to many teachers in the Department of Applied Chemistry & Chemical Technology, the University of Dhaka, Bangladesh, specially my M. S. thesis supervisor and respected teacher **Prof. Dr. A. N. M. Hamidul Kabir** (Dhaka University, Bangladesh). His involvement with his originality has triggered and nourished my intellectual maturity that I will benefit from, for a long time to

come. I owe my deepest gratitude to **Dr. M. A. Khan** (Atomic Energy Inst. Bangladesh) for his advice and his willingness to share his bright thoughts with me.

Collective and individual acknowledgments are also owed to my colleagues at Seki Laboratory in the Department of Molecular Design and Enginnering whose present somehow perpetually refreshed, helpful, and memorable. Many thanks go in particular to **Dr. A. B. Imran, M. Honda** and **N. Kumano** for helping me to learn basic experimental procedures and for showing me the operational techniques of some important instrument. I would like to thank **M. Hara, H. Suzuki, M. N. Huda** and **Y. Gotoh** for their support and encouragement throughout my research work.

Words fail me to express my appreciation to my entire lab mates and staffs, whose dedication, love and persistent confidence in me, has taken the load off my shoulder. I owe them for being unselfishly let their intelligence, passions, and ambitions collide with mine. It's an honor for me to show my deepest gratitude to them for giving me such a pleasant time when working together.

Last, but not least, I thank my family: my parents, for educating me with aspects from both arts and sciences, for unconditional support and prayers. I am grateful to my brothers for listening to my complaints and frustrations, and for believing in me.

Finally, I would like to thank everybody who was important to the successful realization of thesis, as well as expressing my apology that I could not mention personally one by one.

For any errors or inadequacies that may remain in this work, of course, the responsibility is entirely my own.

March, 2010

Mohammad Harun-ur-Rashid

Molecular Assembly System Laboratory

Department of Molecular Design & Engineering

Graduate School of Engineering, Nagoya University

Furo-cho, Chikusa-ku, Nagoya, Aichi 464-8603, Japan

Abstract

Fabrication of Amorphous Microstructure for Distortion Free Structural Color

Mohammad Harun-ur-Rashid, Department of Molecular Design & Engineering, Graduate School of Engineering, Nagoya University ,Nagoya, Japan

It has been demonstrated for the first time that three-dimensional colloidal amorphous arrays, prepared from two different submicron-sized silica particles, are able to exhibit a specific structural color that remains unchanged during the alternation of viewing angle. The morphology and the optical nature of the arrays were analyzed by scanning electron microscopy (SEM) combined with image processing techniques, optical microscopy, and spectroscopy. Transmittance spectra and digital optical microscopic images obtained from different viewing angles show that the structural color is angle independent, whereas an SEM image processed by a custom image analysis strategy depicts the presence of an amorphous structure along with a pseudo-gap in the arrays. The refractive index in amorphous photonic material changes identically in all directions. This isotropic feature of the dielectric distribution leads to wavelength-selective light scattering. As a result, the structural color of the colloidal amorphous arrays is independent of the direction of incident light.

Table of Contents

CHAPTER 5

List of Figures (with page number)

CHAPTER 1

GENERAL INTRODUCTION

1. General Introduction

Functional materials possessing structural color have a potential for next-generation multimedia such as a full-color paperlike display,[1–8] because they can be very energy-efficient, less subject to light fading, and good viewable in both bright sunlight and dimly lit environments. Photonic crystals, consisting of dielectric microstructures with periodicity of roughly half the visible light wavelength, can be strong candidates, because they reveal brilliant structural colors based on a pseudo- or complete photonic band gap (PBG) by Bragg reflection of light. Colloidal crystals composed of submicron sized spherical monodispersed particles[9–12] and microphase-separated block copolymers[13–14] by self-assembly approaches have been under intense study for the preparation of photonic crystals as full color pixels. The structural color from these photonic crystals can be varied using external stimuli such as electric field and optical irradiation, due to the change in the periodicity or refraction index, without the need for color filters or optical elements.[4–8] However, the change in hue with angle of observation or illumination, observed from these photonic crystals, can be major development issue for full-color displays with a wide viewing angle.[1–3]

Here a facile method which is very simple in operation, relatively cheap, less time consuming, to obtain structural colored materials without angle dependence, has been discussed in this thesis. In general, the requirement for materials to exhibit PBG must be alternating regions with high dielectric contrast. The dielectric lattices with periodicity on the order of light wavelength can manipulate light on the basis of Bragg reflection. In Bragg reflection, the wavelength of reflected light is governed by the lattice spacing, refractive index, and angle of incidence. Judging from the

conventional idea of PBG, the structural color variation with observable and incident angles seems to be an unavoidable matter.

In natural world, however, there exists many types of structural colored materials without angle dependence, arise from the interaction between light and various microstructures. The wings of *morpho* butterflies are well-known example exhibiting brilliant blue structural colors without angle dependence.[15] The structural color originates mainly from light interference within separated lamella structure on each scale on a wing. The ridge height of the separated lamella is irregular: the irregularity destroys the interference among neighboring lamellae, which results in the diffuse and uniformly distributed reflectance in angle. The *morpho* butterflies acquired angle independent structural color of their wings due to the structural irregularity coexistent with the structural regularity in microscopic region on each scale. The microstructure of the scale on a *morpho* butterfly wing can be artificially manufactured by focused ion-beam chemical-vapor-deposition.[16] The fabricated structure has nearly the same shape and size as *morpho* butterfly scales, and shows a reflection spectrum with peak intensity near 440 nm and the intensity curves are very similar shape for various incidence angles of light. However, even the fabrication of a tiny chip of the artificial *morpho* butterfly scale would be extremely expensive using this technique.

In other examples, the microphase-separated structures in avian feather barbs also possess angle independent structural colors. One of the simplest structure is the amorphous array of β-keratin particles, phase separated from cytoplasm within medullary cells.[17] The intensity and position of the peak of the reflectance spectra from the amorphous array are relatively constant over incident angles from normal to 65°. Each photon has a high probability of being scattered by the amorphous array,

resulting in a significant contribution of multiply scattered photons to the backscattering signal.

The amorphous particle arrays consisting of two different submicron-sized monodispersed spherical silica particles has been fabricated in order to obtain structural colored materials without angle dependence, which is the artificially-imitated amorphous array of β-keratin particles in avian feather barbs. The amorphous arrays obtained reveal angle independent matte structural colors depending on the weight ratio of the two different sized silica particles. The pseudo-gap can be observed from the measurement of transmission spectra of these samples and the peak positions of the pseudo-gap are virtually constant over incident angle from 0° to 40°.

To have a clear idea of the total work some key words should be described elaborately such as structural color, amorphous microstructure, angle dependence or the distortion of structural color. Discussions on those important terms have been mentioned in this chapter.

1.1. Color

The world is full of light. Visible light is made of seven wavelength groups. Color is the visual perceptual property corresponding in humans to the categories called *red*, *yellow*, *blue* and others. Color derives from the spectrum of light (distribution of light energy versus wavelength) interacting in the eye with the spectral sensitivities of the light receptors. Color categories and physical specifications of color are also associated with objects, materials, light sources, etc., based on their physical properties such as light absorption, reflection, or emission spectra. By defining a color space, colors can be identified numerically by their coordinates.

Because perception of color stems from the varying sensitivity of different types of cone cells in the retina to different parts of the spectrum, colors may be defined and quantified by the degree to which they stimulate these cells. These physical or physiological quantifications of color, however, do not fully explain the psychophysical perception of color appearance.[18-23]

When a matter is illuminated with white light, we see a specific color if the reflected light of a particular wavelength range is visible to our eyes. There are two ways to eliminate the other wavelengths of light: one is the case where the light is absorbed in a material, which is usually the case for ordinary coloration mechanism in colored materials such as pigments, dyes, and metals. In these materials, the illuminating light interacts with electrons within the material and excites them to higher excited states by the virtue of energy consumption of light.

The other is the case where the light is reflected, scattered, and deflected not to reach the eyes under the presence of a specific structure. The coloration in this case is based on a purely physical operation of light that interacts with various types of spatial inhomogeneity. So there are two types of color, one is pigmentary color and the other is structural color.

1.1.1. Pigmentary Color

A pigment is a material that changes the color of reflected or transmitted light as the result of wavelength-selective absorption. This physical process differs from fluorescence, phosphorescence, and other forms of luminescence, in which a material emits light. Many materials selectively absorb certain wavelengths of light. Materials that humans have chosen and developed for use as pigments usually have special

properties that make them ideal for coloring other materials. A pigment must have a high tinting strength relative to the materials it colors. It must be stable in solid form at ambient temperatures.

Pigments appear the colors they are because they selectively reflect and absorb certain wavelengths of light. White light is a roughly equal mixture of the entire visible spectrum of light. When this light encounters a pigment, some wavelengths are absorbed by the chemical bonds and substituents of the pigment and others are reflected. This new reflected light spectrum creates the appearance of a color. Ultramarine reflects blue light, and absorbs other colors. Pigments, unlike fluorescent or phosphorescent substances, can only subtract wavelengths from the source light, never add new ones. The appearance of pigmentary color is intimately connected to the color of the source light. Sunlight has a high color temperature, and a fairly uniform spectrum, and is considered a standard for white light. Artificial light sources tend to have great peaks in some parts of their spectrum, and deep valleys in others. Viewed under these conditions, pigments will appear different colors.

1.1.2. Structural Color

The scientific definition of structural color has not yet been settled and its characteristics are often referred to in contrast to pigmentary color.[24-30] When a substance is illuminated with white light, we see a specific color if the reflected light of only a particular wavelength range is visible to our eyes. There are two ways to eliminate the other wavelengths of light: one is the case where the light is absorbed in a material, which is usually the case for ordinary coloration mechanisms in colored materials such as in pigments, dyes and metals. In these materials, the illuminating light interacts with electrons and excites them to higher excited states by virtue of the

energy consumption of light. The color in this case is anyway caused by the exchange of energies between light and the electrons. The other is the case where light is reflected and/or deflected from reaching the eyes owing to the presence of structure. The coloration in this case is based on a purely physical operation of light that interacts with various types of spatial inhomogeneity. Thus, it does not essentially involve loss of light energy. In this sense, fundamental optical processes such as reflection, refraction, interference, diffraction and scattering can become sources of structural colors. In fact, even a simple prism should be categorized into this type of structural color, because the light waves with different wavelengths are deflected differently by virtue of its wavelength-dependent refractive index. In general, the mechanisms of structural colors are categorized into several optical phenomena such as thin-film interference, multilayer interference, diffraction grating and photonic crystals. However, most of the structural colors appearing in nature somehow utilize special mechanisms to enhance the colorations by combining these optical phenomena. *Structural color* and *iridescence* are two major keywords for these phenomena and seem to be used widely in an equivalent sense. [31-36] However, the term iridescence should be used somewhat in a restricted sense when the color apparently changes with the viewing angle. For example, thin-film interference is generally iridescent, while light scattering is usually non-iridescent but of a structural origin.

1.1.3. Typical Optical Processes Producing Structural Colors

1.1.3.1. Thin-film Interference

If two waves are in the same place at the same time, they combine with each other to produce a resultant wave in accordance with the principle of superposition.

This effect is called interference. Let a plane wave of light be incident on a thin film of thickness d and refractive index n_b with the angles of incidence and refraction as θ_a and θ_b. The light reflected at the two surfaces interferes with each other. In general, the interference condition differs according to whether the thin film is attached to a material having a higher refractive index or not. The former is the case for the anti-reflective coating on glasses, while a typical example of the latter is a soap bubble. The reason for the difference is that the reflection at a surface changes its phase by 180^{o}, when the light is incident from a material with a smaller refractive index to that with a higher one, while it does not in the inverse case. In the soap-bubble case, the condition for constructive interference becomes

$$2n_b d \cos \theta_b = (m - 1/2)\, \lambda, \tag{1}$$

where λ is the wavelength giving the maximum reflectivity and m is an integer. On the other hand, absolutely the same condition is applied to the anti-reflective coating where destructive interference occurs. The constructive interference in the latter case is obtained simply as

$$2n_b d \cos \theta_b = m\lambda. \tag{2}$$

In this treatment, we usually consider only one-time reflection at each surface. However, when the material shows higher reflectance at the interface, multiple reflections considerably affect the interference. An exact calculation considering such multiple reflections gives the amplitude reflectivity and transmittance as

$$r = r_{ab} + t_{ab} r_{bc} t_{ba} e^{i\varphi} + \cdots = r_{ab} + t_{ab} r_{bc} t_{ba} e^{i\varphi} \kappa, \tag{3}$$

$$t = t_{ab} t_{bc} e^{i\varphi/2} + t_{ab} r_{bc} r_{ba} t_{bc} e^{3i\varphi/2} + \cdots = t_{ab} t_{bc} e^{i\varphi/2} \kappa, \tag{4}$$

where $\kappa = 1/(1 - r_{bc} r_{ba} \exp[i\varphi])$ and $\varphi = 4\pi n_b d \cos \theta_b / \lambda$. r_{ab} and t_{ab} are the amplitude reflectivity and transmittance at an interface incident from a to b, respectively, and are obtained from Fresnel's law. Then, the power reflectivity and transmittance are given

as $R = |r|^2$ and $T = (n_c/n_a)|t|^2$ with $R + T = 1$ as long as the refractive indices are real. It is easily shown that $\kappa = 1$ with $t_{ab}t_{ba} = 1$ and $|r_{ab}| = |r_{bc}|$ corresponds to one-time reflection at each surface. It is clear that the reflectivity is rather low in each case and smoothly changes with the wavelength. Thus simple thin-film interference gives only weak dependence on the wavelength with low reflectance.

If the thickness of the film becomes larger, regular multiple peaks appear in the reflection spectrum as a consequence of the higher-order interference with $m > 1$. These peaks in a visible region cause a special effect called *non-spectral color* to human vision in contrast to an ordinary *spectral color*, i.e. a single wavelength of light is perceived in the eye. The non-spectral color is deeply connected with the spectral sensitivities of vision and is explained in terms that more than two color-receptors among three are sensed simultaneously. Violet is a spectral color, but purple and magenta are non-spectral colors. White is also a non-spectral color, where all three color-receptors are sensed. The multiple peak in thin-film interference can become an origin of non-spectral color. A typical example has been recently found in the neck feather of the rock dove[37,38], which specifically shows green/purple two-color iridescence. It is expected that the angular dependence is more pronounced for the higher order interference of $m > 1$ than that of $m = 1$, which makes the iridescent effect more vivid.

In figure 1.1(a) the interference of light through thin layer and (b) the iridescent structural color displayed by the soap bubble due to the interference of light have been shown.

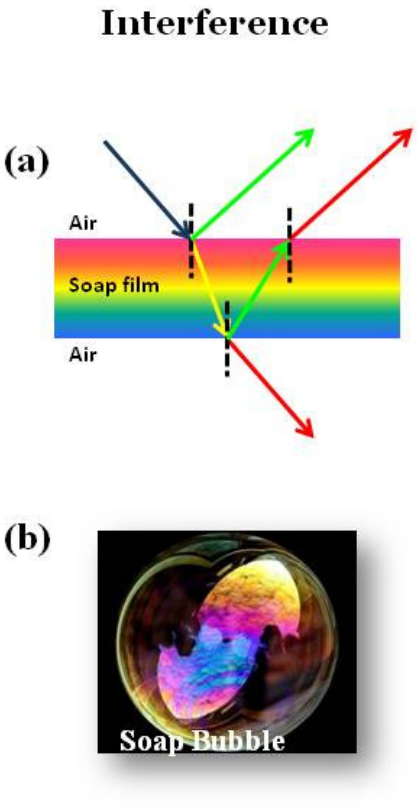

Figure 1.1. (a) the interference of light through thin layer. (b) iridescent structural color displayed by the soap bubble due to the interference of light

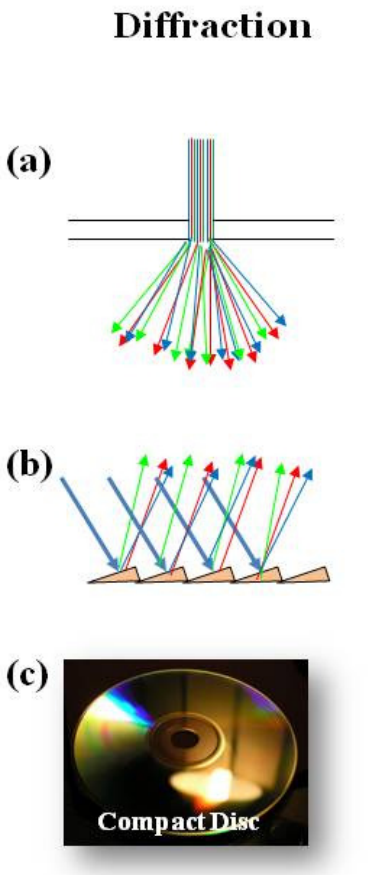

Figure 1.2. (a) the diffraction of light through pin-hole. (b) the diffraction of light due to the patterned surface. (c) iridescent structural color displayed by the compact disk due to the diffraction of light

1.1.3.2. Multilayer Interference

Multilayer interference is qualitatively understood in terms of a pair of thin layers piling periodically. Consider two layers designated as A and B with thicknesses d_A and d_B, and refractive indices n_A and n_B, respectively. It is assumed that $n_A > n_B$ for the present. If it is considered a certain pair of AB layers, the phases of the reflected light both at the upper and lower B–A interfaces change by 180^o. Thus a relation similar to the anti-reflective coating of equation (2) is applicable as

$$2(n_A d_A \cos \theta_A + n_B d_B \cos \theta_B) = m\lambda, \quad (5)$$

for constructive interference with the angles of refraction in the A and B layers as θA and θ_B. On the other hand, if we consider only the A layer within the AB layer, the phase of the reflected light does not change at an A–B interface. Thus if a soap-bubble relation, $2n_A d_A \cos \theta_A = (m' - 1/2)\lambda$, is further satisfied for the same wavelength, the reflected light from the A–B interface adds to that from the B–A interfaces and the multilayer gives the maximum reflectivity. In particular, the relations with $m = 1$ and $m' = 1$ correspond to the lowest-order case, where the optical path lengths, defined as the length multiplied by the refractive index, for A and B layers are equal to each other. Land called this case the *ideal multilayer* [39]. On the other hand, if the thickness of the A layer does not satisfy the soap-bubble relation, while the sum of the A and B layers satisfies equation (5), the reflection at the A–B interface works destructively and the peak reflectivity decreases. This case is the *non-ideal multilayer*.

Nowadays, the reflectivity and transmittance of a multilayer with arbitrary refractive indices and thicknesses without any periodicity are easily calculated through a transfer matrix method [40-42], in addition to the well-known iterative and Huxley's methods [43]. Since the details of these methods have been fully described before, here we describe only the results calculated by the above methods.

1.1.3.3. Diffraction of Light and Diffraction Grating

Diffraction is normally taken to refer to various phenomena which occur when a wave encounters an obstacle. It is described as the apparent bending of waves around small obstacles and the spreading out of waves past small openings. Similar effects are observed when light waves travel through a medium with a varying refractive index or a sound wave through one with varying acoustic impedance. Diffraction occurs with all waves, including sound waves, water waves, and electromagnetic waves such as visible light, x-rays and radio waves. As physical objects have wave-like properties (at the atomic level), diffraction also occurs with matter and can be studied according to the principles of quantum mechanics.

While diffraction occurs whenever propagating waves encounter such changes, its effects are generally most pronounced for waves where the wavelength is on the order of the size of the diffracting objects. If the obstructing object provides multiple, closely-spaced openings, a complex pattern of varying intensity can result. This is due to the superposition, or interference, of different parts of a wave that traveled to the observer by different paths.

The formalism of diffraction can also describe the way in which waves of finite extent propagate in free space. For example, the expanding profile of a laser beam, the beam shape of a radar antenna and the field of view of an ultrasonic transducer are all explained by diffraction theory.

The effects of diffraction can be regularly seen in everyday life. The most colorful examples of diffraction are those involving light; for example, the closely spaced tracks on a CD or DVD act as a diffraction grating to form the familiar

rainbow pattern we see when looking at a disk. This principle can be extended to engineer a grating with a structure such that it will produce any diffraction pattern desired; the hologram on a credit card is an example. Diffraction in the atmosphere by small particles can cause a bright ring to be visible around a bright light source like the sun or the moon. A shadow of a solid object, using light from a compact source, shows small fringes near its edges. The speckle pattern which is observed when laser light falls on an optically rough surface is also a diffraction phenomenon. All these effects are a consequence of the fact that light propagates as a wave.

Diffraction can occur with any kind of wave. Ocean waves diffract around jetties and other obstacles. Sound waves can diffract around objects, which is why one can still hear someone calling even when hiding behind a tree. Diffraction can also be a concern in some technical applications; it sets a fundamental limit to the resolution of a camera, telescope, or microscope.

In figure 1.2(a) the diffraction of light through pin-hole and (b) The diffraction of light due to the patterned surface and (c) iridescent structural color displayed by the compact disk due to the diffraction of light.

1.1.3.4. Light interactions by Microstructures

1.1.3.4.1. Crystalline Structures

If small identical particles are regularly arranged like a crystal, light scattered from each particle interferes and radiates secondary emission in regular directions. The theoretical treatment of this type of scattering was first developed in the field of x-ray diffraction, in which the theory considering only one-time scattering from each particle is called ‘kinematic theory’, whereas that considering multiple scattering is called ‘dynamical theory’. These approaches have been extended to a system

consisting of much larger particles with various crystal structures and a new research field called photonics or photonic crystals has opened. The interaction of electromagnetic waves with periodic microstructures has been extensively studied in conjunction with coming new photon technology, which prevails over electronics based on semiconductor technology. However, the theoretical treatments have not been changed basically from the dynamical theory of x-ray diffraction except that accurate results are obtained through computer calculation.

In figure 1.4, (a) crystalline microstructure and (b) iridescent structural color of colloidal crystal have been shown.

1.1.3.4.2. Quasi-crystalline Structures

Quasicrystals are structural forms that are both ordered and nonperiodic. They form patterns that fill all the space but lack translational symmetry. Classical theory of crystals allows only 2, 3, 4, and 6-fold rotational symmetries, but quasicrystals display symmetry of other orders (folds). They can be said to be in a state intermediate between crystal and glass. Just like crystals, quasicrystals produce modified Bragg diffraction, but where crystals have a simple repeating structure, quasicrystals are more complex.

Aperiodic tilings were discovered by mathematicians in the early 1960s, but some twenty years later they were found to apply to the study of quasicrystals. The discovery of these aperiodic forms in nature has produced a paradigm shift in the fields of crystallography and solid state physics. Quasicrystals had been investigated and observed earlier but until the 80s they were disregarded in favor of the prevailing views about the atomic structure of matter.

Roughly, an ordering is non-periodic if it lacks translational symmetry, which means that a shifted copy will never match exactly with its original. The more precise mathematical definition is that there is never translational symmetry in more than $n - 1$ linearly independent directions, where n is the dimension of the space filled; i.e. the three-dimensional tiling displayed in a quasicrystal may have translational symmetry in two dimensions. The ability to diffract comes from the existence of an indefinitely large number of elements with a regular spacing, a property loosely described as long-range order. Experimentally the aperiodicity is revealed in the unusual symmetry of the diffraction pattern, that is, symmetry of orders other than 2, 3, 4, or 6. The first officially reported case of what came to be known as quasicrystals was made by Dan Shechtman and coworkers in 1984. The distinction between quasicrystals and their corresponding mathematical models (e.g. the three-dimensional version of the Penrose tiling) need not be emphasized.

Each class of nanostructure is isotropic and has a pronounced characteristic length scale of variation in composition. These local structural correlations lead to strong backscattering over a narrow range of optical frequencies and a variation with angle of incidence.

1.1.3.4.3. Amorphous Micro-structures

An "amorphous solid" is a solid in which there is no long-range order of the positions of the atoms. (Solids in which there is long-range atomic order are called crystalline solids or morphous). Most classes of solid materials can be found or prepared in an amorphous form. For instance, common window glass is an amorphous

solid, many polymers (such as polystyrene) are amorphous, and even foods such as cotton candy are amorphous solids.

In principle, given a sufficiently high cooling rate, any liquid can be made into an amorphous solid. Cooling reduces molecular mobility. If the cooling rate is faster than the rate at which molecules can organize into a more thermodynamically favorable crystalline state, then an amorphous solid will be formed. Because of entropy considerations, many polymers can be made amorphous solids by cooling even at slow rates. In contrast, if molecules have sufficient time to organize into a structure with two- or three-dimensional order, then a crystalline (or semi-crystalline) solid will be formed. Water is one example. Because of its small molecular size and ability to quickly rearrange, it cannot be made amorphous without resorting to specialized hyperquenching techniques.

Amorphous materials can also be produced by additives which interfere with the ability of the primary constituent to crystallize. For example, addition of soda to silicon dioxide results in window glass, and the addition of glycols to water results in a vitrified solid.

Some materials, such as metals, are difficult to prepare in an amorphous state. Unless a material has a high melting temperature (as ceramics do) or a low crystallization energy (as polymers tend to), cooling must be done extremely rapidly. As the cooling is performed, the material changes from a supercooled liquid, with properties one would expect from a liquid state material, to a solid. The temperature at which this transition occurs is called the glass transition temperature or T_g.

It is difficult to make a distinction between truly amorphous solids and crystalline solids if the size of the crystals is very small. Even amorphous materials have some short-range order at the atomic length scale due the nature of chemical bonding. Furthermore, in very small crystals a large fraction of the atoms are located at or near the surface of the crystal; relaxation of the surface and interfacial effects distort the atomic positions, decreasing the structural order. Even the most advanced structural characterization techniques, such as x-ray diffraction and transmission electron microscopy, have difficulty in distinguishing between amorphous and crystalline structures on these length scales.

The transition from the liquid state to the glass, at a temperature below the equilibrium melting point of the material, is called the glass transition. The glass transition temperature is approximately the temperature at which the viscosity of the liquid exceeds a certain value. The transition temperature depends on cooling rate, with the glass transition occurring at higher temperatures for faster cooling rates. The precise nature of the glass transition is the subject of ongoing research. While it is clear that the glass transition is not a first-order thermodynamic transition (such as melting), there is debate as to whether it is a higher-order transition, or merely a kinetic effect. This class of nanostructure is isotropic and has a pronounced characteristic length scale of variation in composition. These local structural correlations lead to strong backscattering over a narrow range of optical frequencies and little variation with angle of incidence.

In figure 1.4, (c) amorphous microstructure and (d) non-iridescent structural color of amorphous microstructure have been shown.

1.1.3.5. Light Scattering

Light scattering is another important source of structural colors. Scattering is a general physical process where some forms of radiation, such as light, sound, or moving particles, are forced to deviate from a straight trajectory by one or more localized non-uniformities in the medium through which they pass. In conventional use, this also includes deviation of reflected radiation from the angle predicted by the law of reflection. Reflections that undergo scattering are often called *diffuse* reflections and unscattered reflections are called *specular* (mirror-like) reflections.

The types of non-uniformities which can cause scattering, sometimes known as *scatterers* or *scattering centers*, are too numerous to list, but a small sample includes particles, bubbles, droplets, density fluctuations in fluids, defects in crystalline solids, surface roughness, cells in organisms, and textile fibers in clothing. The effects of such features on the path of almost any type of propagating wave or moving particle can be described in the framework of scattering theory.

The light scattering by a particle much smaller than the wavelength of light is called Rayleigh scattering. The color of the blue sky is one of the examples of Rayleigh scattering of light. When the size of the particle becomes comparable or larger than the wavelength of light, then it is Mie scattering of light. In this case, a plane wave of light illuminates a dielectric sphere, by which light is scattered after reflection, refraction and diffraction.

In figure 1.3(a) Rayleigh scattering of light, (b) blue color of sky due to Rayleigh scattering, (c) Mie scattering and (d) red color of sky due to Mie scattering have been shown.

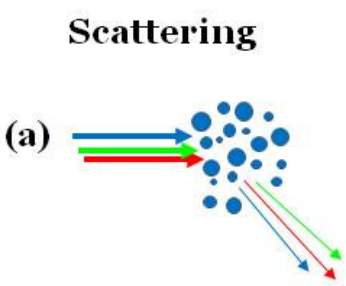

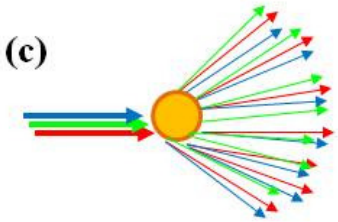

Figure 1.3. (a) Rayleigh scattering of light, (b) blue color of sky due to Rayleigh scattering, (c) Mie scattering and (d) red color of sky due to Mie scattering.

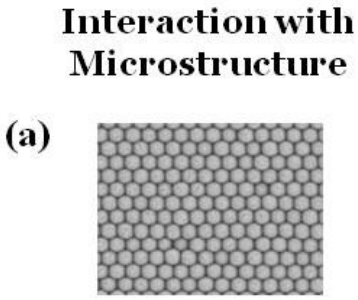

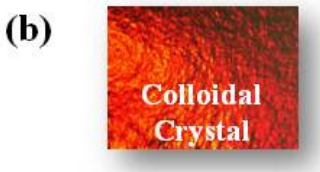

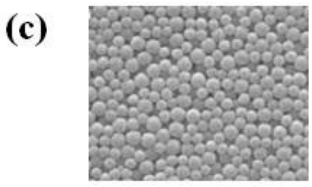

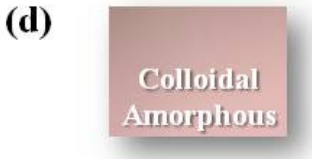

Figure 1.4. (a) crystalline microstructure, (b) iridescent structural color of colloidal crystal, (c) amorphous microstructure and (d) non-iridescent structural color of amorphous microstructure.

1.2. Distortion of Structural Color

A distortion is the alteration of the original shape (or other characteristic) of an object, image, sound, waveform or other form of information or representation. Here distortion of structural color means the change in the hue of the color due the change of the angle of illumination or the viewing angle or the both. Distortion of color is a great issue where a specific color carries a specific signal. Especially in the case of display purpose distortion free color is required to devise display with a wide viewing angle. In liquid crystal display (LCD) technology, the more oblique the viewing angle the larger the changes in the physical image. But to retain the image quality better distortion free structural color has a great significance. To get a clear idea about the distortion of structural color two major key words could be discussed elaborately. One is iridescent color and another one is non-iridescent color.

1.2.1. Iridescent Color

Iridescence (also known as goniochromism) is generally known as the property of certain surfaces which appear to change color as the angle of view changes. So the iridescent color means the color which apparently changes with viewing angles. Iridescence may be seen commonly in soap bubbles, butterfly wings and sea shells. Iridescence is an optical phenomenon of surfaces in which hue changes in correspondence with the angle from which a surface is viewed.

Iridescence is caused by multiple reflections from multi-layered, semi-transparent surfaces in which phase shift and interference of the reflections modulates the incident light (by amplifying or attenuating some frequencies more than others).

This process is the functional analog of selective wavelength attenuation as seen with the Fabry-Pérot interferometer.

1.2.2. Non-iridescent Color

Non-iridescent color is that color which remains unchanged at different viewing angle. Color produced by the scattering of light is a type of non-iridescent color.

1.3. References

[1] Y. Takeoka, M. Honda, T. Seki, M. Ishii, H. Nakamura, *ACS Appl. Mater. & Interfaces.* **2009**, *1*, 982-986.

[2] M. Harun-Ur-Rashid, T. Seki, Y. Takeoka, *Chem. Rec.* **2009**, *9*, 87-105.

[3] K. Ueno, A. Inaba, Y. Sano, M. Kondoh, M. Watanabe, *Chem. Commun.* **2009**, 3603-3605.

[4] K. Matsubara, M. Watanabe, Y. Takeoka, *Angew. Chem., Int. Ed.* **2007**, *46*, 1688-1692.

[5] K. Ueno, K. Matsubara, M. Watanabe, Y. Takeoka, *Adv. Mater.* **2007**, *19*, 2807-2812.

[6] K. Ueno, J. Sakamoto, Y. Takeoka, M. Watanabe, *J. Mater. Chem.* **2009**, *19*, 4778-4783.

[7] A. C. Arsenault, D. P. Puzzo, I. Manners, G. A. Ozin, *Nat. Photonics* **2007**, *1*, 468-472.

[8] S. H. Kim, S. J. Jeon, W. C. Jeong, H. S. Park, S. M. Yang, *Adv. Mater.* **2008**, *20*, 4129-4134.

[9] A. S. Dimitrov, K. Nagayama, *Langmuir* **1996**, *12*, 1303-1311.

[10] Z. Z. Gu, A. Fujishima, O. Sato, *Chem. Mater.* **2002**, *14*, 760-765.

[11] J. F. Bertone, P. Jiang, K. S. Hwang, D. M. Mittleman, V. L. Colvin, *Phys. Rev. Lett.* **1999**, *83*, 300-303.

[12] R. Mayoral, J. Requena, J. S. Moya, C. Lopez, A. Cintas, H. Miguez, F. Meseguer, L. Vazquez, M. Holgado, A. Blanco, *Adv. Mater.* **1997**, *9*, 257-260.

[13] J. Yoon, W. Lee, E. L. Thomas, *Macromol.* **2008**, *41*, 4582-4584.

[14] P. D. Hustad, G. R. Marchand, E. I. Garcia-Meitin, P. L. Roberts, J. D. Weinhold, *Macromol.* **2009**, *42*, 3788-3794.

[15] S. Kinoshita, S. Yoshioka, K. Kawagoe, *Proc. Royal Soc. London Series B-Biological Sci.* **2002**, *269*, 1417-1421.

[16] K. Watanabe, T. Hoshino, K. Kanda, Y. Haruyama, S. Matsui, *Jpn. J. Appl. Phys. Part 2-Lett. & Exp. Lett.* **2005**, *44*, L48-L50.

[17] E. R. Dufresne, H. Noh, V. Saranathan, S. G. J. Mochrie, H. Cao, R. O. Prum, *Soft Matter* **2009**, *5*, 1792-1795.

[18] Craig F. Bohren (2006). *Fundamentals of Atmospheric Radiation: An Introduction with 400 Problems*. Wiley-VCH. ISBN 3527405038.

[19] Berlin, B. and Kay, P., *Basic Color Terms: Their Universality and Evolution*, Berkeley: University of California Press, 1969.

[20] Hermann von Helmholtz, *Physiological Optics – The Sensations of Vision*, 1866, as translated in *Sources of Color Science*, David L. MacAdam, ed., Cambridge: MIT Press, 1970.

[21] Palmer, S.E. (1999). *Vision Science: Photons to Phenomenology*, Cambridge, MA: MIT Press. ISBN 0-262-16183-4. Judd, Deane B.; Wyszecki, Günter (1975). *Color in Business, Science and Industry*. Wiley Series in Pure and Applied Optics (third edition ed.). New York: Wiley-Interscience. p. 388. ISBN 0471452122.

[22] "Under well-lit viewing conditions (photopic vision), cones ...are highly active and rods are inactive." Hirakawa, K.; Parks, T.W. (2005). "Chromatic Adaptation and White-Balance Problem". *IEEE ICIP*. doi:10.1109/ICIP.2005.1530559.

[23] Jameson, K. A., Highnote, S. M., & Wasserman, L. M. (2001). "Richer color experience in observers with multiple photopigment opsin genes." *Psychonomic Bulletin and Review* 8 (2): 244–261. doi:10.1038/351652a0.

[24] S. Kinoshita, S. Yoshika and J. Miyazaki, *Rep. Prog. Phys.* **71** (2008), 076401 (30p).

[25] Parker A R 1998 *J. Exp. Biol.* **201** 2343–7.

[26] Srinivasarao M 1999 *Chem. Rev.* **99** 1935–61.

[27] Parker A R 2000 *J. Opt. A: Pure Appl. Opt.* **2** R15–R28.

[28] Vukusic P and Sambles J R 2003 *Nature* **424** 852–5.

[29] Parker A R 2004 *Phil. Trans. R. Soc. Lond.* A **362** 2709–20.

[30] Kinoshita S and Yoshioka S 2005 *ChemPhysChem* **6** 1442–59.

[31] Kinoshita S, Yoshioka S and Kawagoe K 2002 *Proc. R. Soc. Lond.* B **269** 1417–21.

[32] Kinoshita S, Yoshioka S, Fuii Y and Okamoto N 2002 *Forma* **17** 103–121.

[33] Berthier S, Charron E and Da Silva A 2003 *Opt. Commun.***228** 349–56.

[34] Yoshioka S and Kinoshita S 2004 *Proc. R. Soc. Lond.* B **271** 581–7.

[35] Plattner L 2004 *J. R. Soc. Interface* **1** 49–59.

[36] Kinoshita S and Yoshioka S 2005 *Structural Colors in Biological Systems—Principles and Applications* ed S Kinoshita *et al* (Osaka: Osaka University Press) pp 113–40.

[37] Yoshioka S and Kinoshita S 2006 *Proc. R. Soc. Lond.* B **273** 129–34.

[38] Yin H, Shi L, Sha J, Li Y, Qin Y, Dong B, Meyer S, Liu X, Zhao L and Zi J 2006 *Phys. Rev.* E **74** 051916.

[39] Yoshioka S, Nakamura E and Kinoshita S 2007 *J. Phys. Soc. Japan* **76** 013801.

[40] Land M F 1972 *Prog. Biophys. Mol. Biol.* **24** 75-106.

[41] Kinoshita S and Yoshioka S 2005 *ChemPhysChem* **6** 1442-59.

[42] Born M and Wolf E 1975 *Principles of Optics: Electromagnetic Theory of Propagation, Interference and Diffraction of Light* 5th edn (New York: Pergamon).

[43] Kinoshita S and Yoshioka S 2005 *Structural Colors in Biological Systems-Principles and Applications* ed S Kinoshita *et al* (Osaka: Osaka University Press) pp 3-26.

[44] Huxley A. F 1968 *J. Exp. Biol.* **48** 227-45.

[45] Sakoda K 2001 *Optical Properties of Photonic Crystals* (Berlin: Springer).

CHAPTER 2

MATERIALS AND METHODS

2.1. Materials

2.1.1. Silica Colloidal Particle

To construct an amorphous structured 3D solid system, silica colloidal particles were used as the basic component, and a doping technique was used. The introduction of two different sized silica colloids at the same time defaces the crystalline arrangement and mutates the long-range order into short-range order. SiO_2 colloidal particles with a diameter of 310 nm were used as the host, and particles with a diameter of 220 nm were used as the guest constituents for this experiment. An aqueous suspension of sub-micrometer-sized silica particles (silica particles with a narrow particle size distribution, dispersed in water, Nippon Shokubai) was obtained and used to prepare close-packed colloidal crystals and colloidal amorphous arrays.

2.2. Methods

2.2.1. Sample Preparation

To construct an amorphous structured 3D solid system, silica colloidal particles (310 nm and 220 nm, Nippon Shokubai) were used as the basic component, and a doping technique was used.[1] The introduction of two different sized silica colloids at the same time defaces the crystalline arrangement and mutates the long-range order into short-range order.[2-18] SiO_2 colloidal particles with a diameter of 310 nm were used as the host, and particles with a diameter of 220 nm were used as the guest constituents for our experiment. Aqueous suspensions of two different sized SiO_2 colloids were mixed by sonication at various mixing ratios and poured onto hydrophilic glass substrates, which were placed in a thermostatic chamber at 60^{o}C for

6 hr and evaporated to dryness. Several samples of colloidal amorphous arrays were prepared by varying the mixing ratio of the two differently sized colloidal suspensions. The compositions of the mentioned samples are summarized in Table 1.

There are many approaches to prepare colloidal crystal.[19-30] The colloidal array, prepared by simple evaporation method consists of only 310 nm silica colloidal particles, is organized into a close-packed arrangement with a long-range order (hereinafter called "colloidal crystal"). While on the contrary the samples prepared by mixing two different sized silica colloidal particles having the diameter of 310 nm and 220 nm with the same method consist of roughly packed silica spheres (hereinafter called "colloidal amorphous"). Figure 2.1 shows the basic procedure for the preparation of colloidal crystal and colloidal amorphous.

The total wt% of colloidal SiO_2 particles depends on the ration of samples as follows:

Total solid content per glass substrate: 1.4 g of sample

Area of glass substrate: 38 x 26 mm

Dried thickness of the samples: approximately 0.5 mm

Suspension 1: 220-nm sized SiO_2 particle in aqueous suspension (28 wt%)→1 mL contains 0.28 g of solid

Suspension 2: 310-nm sized SiO_2 particle in aqueous suspension (36 wt %)→1 mL contains 0.36 g of solid

Colloidal amorphous array M1 (10% 220-nm particles and 90% 310-nm particles):

Suspension 1, 0.5 mL= 0.14 g of 220-nm particles

Suspension 2, 3.5 mL = 1.26 g of 310-nm particles

The total wt% of the colloidal SiO_2 particles is 35.

Colloidal amorphous array M2 (20% 220-nm particles and 80% 310-nm particle s):

Suspension 1, 1.0 mL = 0.28 g of 220-nm particles

Suspension 2, 3.0 mL = 1.12 g of 310-nm particles

The total wt% of the colloidal SiO_2 particles is 35.

Colloidal amorphous array M3 (30% 220-nm particles and 70% 310-nm particle s):

Suspension 1, 1.5 mL = 0.42 g of 220-nm particles

Suspension 2, 2.7 mL = 0.98 g of 310-nm particles

The total wt% of colloidal SiO_2 particles is 33.3.

Colloidal amorphous array M4 (40% 220-nm particles and 60% 310-nm particle s):

Suspension 1, 2.0 mL = 0.56 g of 220-nm particles

Suspension 2, 2.3 mL = 0.84 g of 310-nm particles

The total wt% of the colloidal SiO_2 particles is 32.6.

Colloidal amorphous array M5 (50% 220-nm particles and 50% 310-nm particle s):

Suspension 1, 2.5 mL = 0.70 g of 220-nm particles

Suspension 2, 2.0 mL = 0.70 g of 310-nm particles

The total wt% of colloidal SiO_2 particles is 31.1.

Colloidal crystal of 310-nm SiO_2

Suspension 2, 3.9 mL = 1.4 g of 310-nm particles

The total wt% of colloidal SiO_2 particles is 35.9.

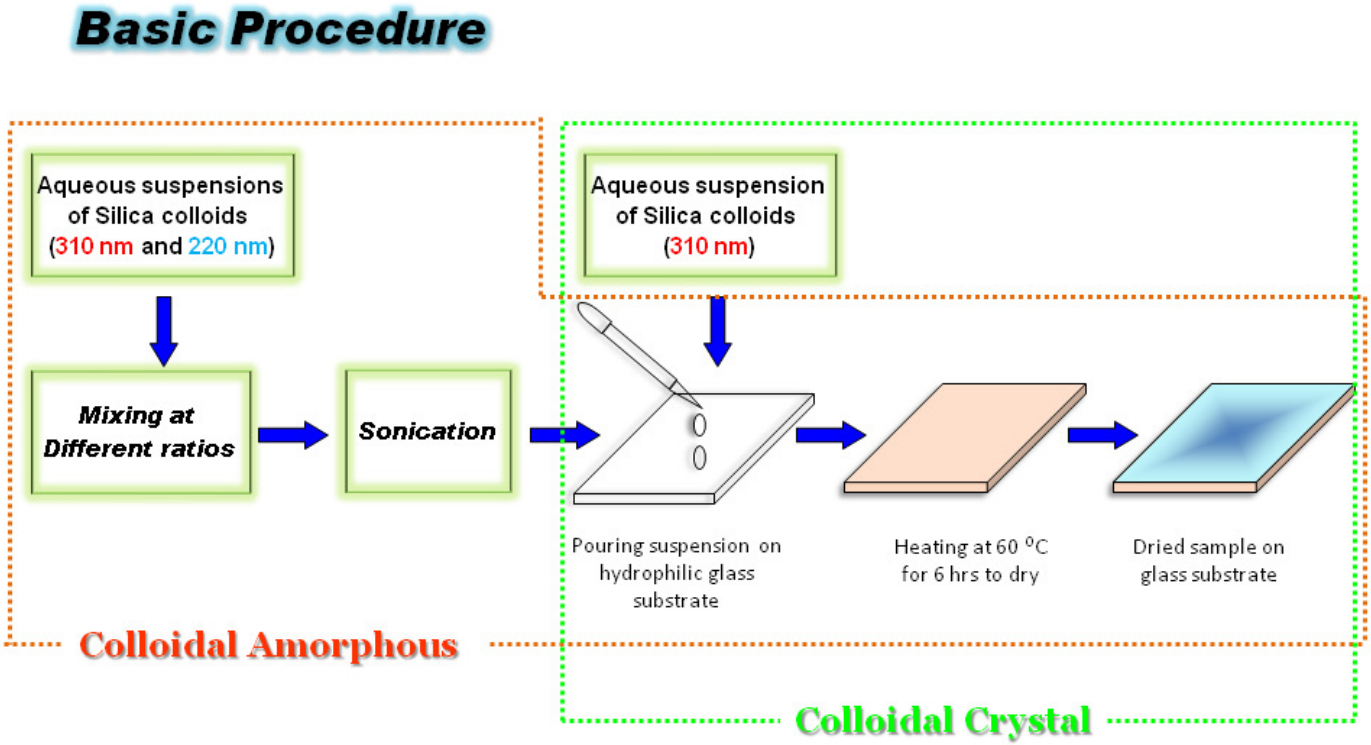

Figure 2.1. Basic procedure for the preparation of colloidal crystal and amorphous microstructure

Sample Composition

Table 1. Summarize the composition of all fabricated samples

Final composition of silica particles in each sample		
Sample	220 nm SiO_2 particle (wt%)	310 nm SiO_2 particle (wt%)
Colloidal Crystal		
CC	0	100
Colloidal Amorphous		
M1	10	90
M2	20	80
M3	30	70
M4	40	60
M5	50	50

Doping Concentration

2.2.2. Scanning Electron Microscopy (SEM)

The scanning electron microscope (SEM) is a type of electron microscope that images the sample surface by scanning it with a high-energy beam of electrons in a raster scan pattern. The electrons interact with the atoms that make up the sample producing signals that contain information about the sample's surface topography, composition and other properties such as electrical conductivity.

The types of signals produced by an SEM include secondary electrons, back-scattered electrons (BSE), characteristic X-rays, light (cathodoluminescence), specimen current and transmitted electrons. Secondary electron detectors are common in all SEMs, but it is rare that a single machine would have detectors for all possible signals. The signals result from interactions of the electron beam with atoms at or near the surface of the sample. In the most common or standard detection mode, secondary electron imaging or SEI, the SEM can produce very high-resolution images of a sample surface, revealing details about less than 1 to 5 nm in size. Due to the very narrow electron beam, SEM micrographs have a large depth of field yielding a characteristic three-dimensional appearance useful for understanding the surface structure of a sample. This is exemplified by the micrograph of pollen shown to the right. A wide range of magnifications is possible, from about 10 times (about equivalent to that of a powerful hand-lens) to more than 500,000 times, about 250 times the magnification limit of the best light microscopes. Back-scattered electrons (BSE) are beam electrons that are reflected from the sample by elastic scattering. BSE are often used in analytical SEM along with the spectra made from the characteristic X-rays. Because the intensity of the BSE signal is strongly related to the atomic number (Z) of the specimen, BSE images can provide information about the

distribution of different elements in the sample. For the same reason, BSE imaging can image colloidal gold immuno-labels of 5 or 10 nm diameter which would otherwise be difficult or impossible to detect in secondary electron images in biological specimens.

Several mixed samples were prepared by varying the doping concentration from 10-50 wt.% and observed their surface structures by scanning electron microscopy (SEM). Using SEM combined with image processing techniques, such as two-dimensional (2D) fast Fourier transform (FFT), we established an independent measure of the ordering of our samples.[31] Because the spatial information in the SEM image can be obtained from a 2D FFT.[32] Figure 2.2 shows the SEM images of colloidal crystal, colloidal amorphous and their corresponding 2D FFT.

2.2.1.1. Sample Preparation for SEM

In this research the arrangement of the colloidal spheres in a crystal structure and amorphous structure was investigated with a scanning electron microscope made by JEOL (JSM 5600). The samples were coated with a 10-nm gold layer, and the SEM was operated at 20 kV.

2.2.3. Two Dimensional (2D) Fast Fourier Transform (FFT)

The 2D FFT function converts spatial information in an optical data image into a mathematically defined frequency domain. This frequency domain maps the rate at which pixel intensities change in the spatial domain. The Fourier transform is also used to transform a continuous time signal into the frequency domain. It describes the continuous spectrum of a nonperiodic time signal. The Discrete Fourier

Transform is used in the case where both the time and the frequency variables are discrete (which they are if digital computers are being used to perform the analysis). Let x(nT) represent the discrete time signal, and let X(mF) represent the discrete frequency transform function. The fast Fourier transform (FFT) is simply a class of special algorithms which implement the discrete Fourier transform with considerable savings in computational time. It must be pointed out that the FFT is not a different transform from the DFT, but rather just a means of computing the DFT with a considerable reduction in the number of calculations required.

Now the question why the 2D FFT was used in this study and the answer is, we established an independent measure of the ordering of our samples by using SEM combined with image processing techniques, such as two-dimensional (2D) fast Fourier transform (FFT),.[31] Because the spatial information in the SEM image can be obtained from a 2D FFT.[32] In this study we describe how to use a two-dimensional fast Fourier transform (2D FFT) approach to measure particle alignment in samples. This image processing function can be coupled with a variety of imaging modalities to assign an objective numerical value of ordering of the particles. A data image of an electron micrograph is composed of pixels that depict the spatial organization of the constituent fibers. The 2D FFT function converts this spatial information into a mathematically defined frequency domain that maps the rate at which pixel intensities change across the original data image. This output image also contains quantitative information concerning the orientation of objects in a data image. We discuss the theory and practice of using the frequency plot of the 2D FFT function to measure samples' anisotropy and identify the principal axis of particle orientation.

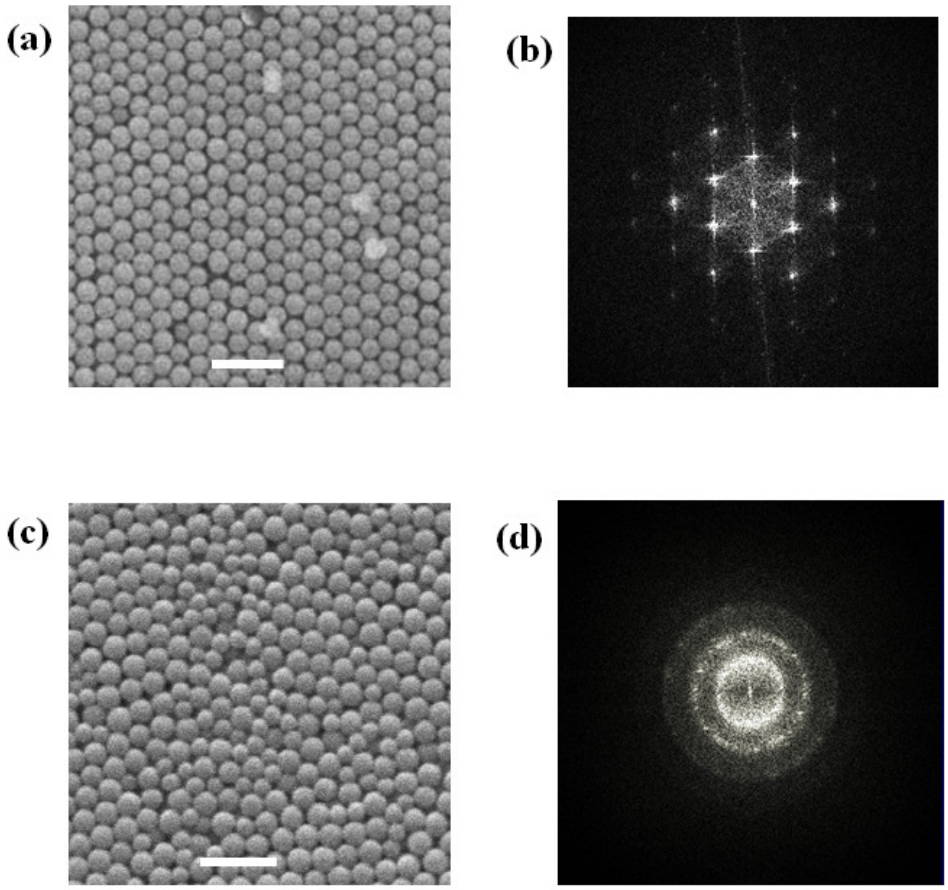

Figure 2.2. Scanning Electron Microscopic (SEM) image of colloidal crystal (a), colloidal amorphous, M1 (c) and (b), (d) are their corresponding 2D fast Fourier transform (FFT), respectively

For analysis, grayscale brightfield microscopic images were captured and converted to an integer power of 2 pixel dimensions (256×256, 512×512, 1024×1024, etc.). If images have been captured in color they must be converted to grayscale for 2D FFT analysis. Care should be taken at the time of image capture to optimize sample illumination; uneven illumination can complicate and introduce error into the alignment analysis. Processing a brightfield data image by 2D FFT produces a frequency plot, or power spectrum. This plot is composed of grayscale pixels that are distributed into a pattern that can be used to measure the degree of fiber alignment present in an original data image. Low-frequency signals correspond to domains within the original microscopy image that contain pixels of similar values, adjacent pixels do not vary to a great extent in intensity. The bulk of this information originates with the background and the overall shape of the image. High-frequency pixels are placed away from the origin and toward the periphery of the frequency plot. This information corresponds to spatial domains that exhibit abrupt changes in pixel intensity. Edges, details and noise in the data image all contribute to the generation of high-frequency pixels. When an image of random fibers is processed by 2D FFT, the resulting frequency plot contains a cluster of white pixels that are concentrated in a symmetrical, circular pattern around the origin.

2.2.4. Autocorrelation Function

The autocorrelation function represents the interrelationship of the contrast function and thereby provides a measure of the translational symmetry in the system. If the particles are organized with a regular distance between first neighbors, the autocorrelation function presents a maximum at the corresponding distance.

To obtain an independent measure of the ordering of our system, the autocorrelation function from scanning electron microscopy (SEM) images was used. The autocorrelation function describes the correlation of the contrast function and gives a measurement of the translational symmetry existing in the system. Generally, SEM images contain repetitive features. For instance, crystal lattices or periodic arrays of microstructures yield multiple occurrences of similar features in one image.

The autocorrelation function is an approach to enhance the interpretation of such data based on the combination of linear correlations of the same feature in one SEM image. First, we obtained an SEM image (Figure 2.3(a)) of our sample. Then, the image was resized to a power of 2 (such as 512 x 512 pixels), and the autocorrelation function (Figure 2.3(b)) was obtained from the SEM image. For measuring the degree of order, we plotted the radial profile of a circular area. Figure 2.3(c) shows the circular area (with center "C" and radius "d") that was considered for plotting the radial profile.

Obtaining an Autocorrelation Function

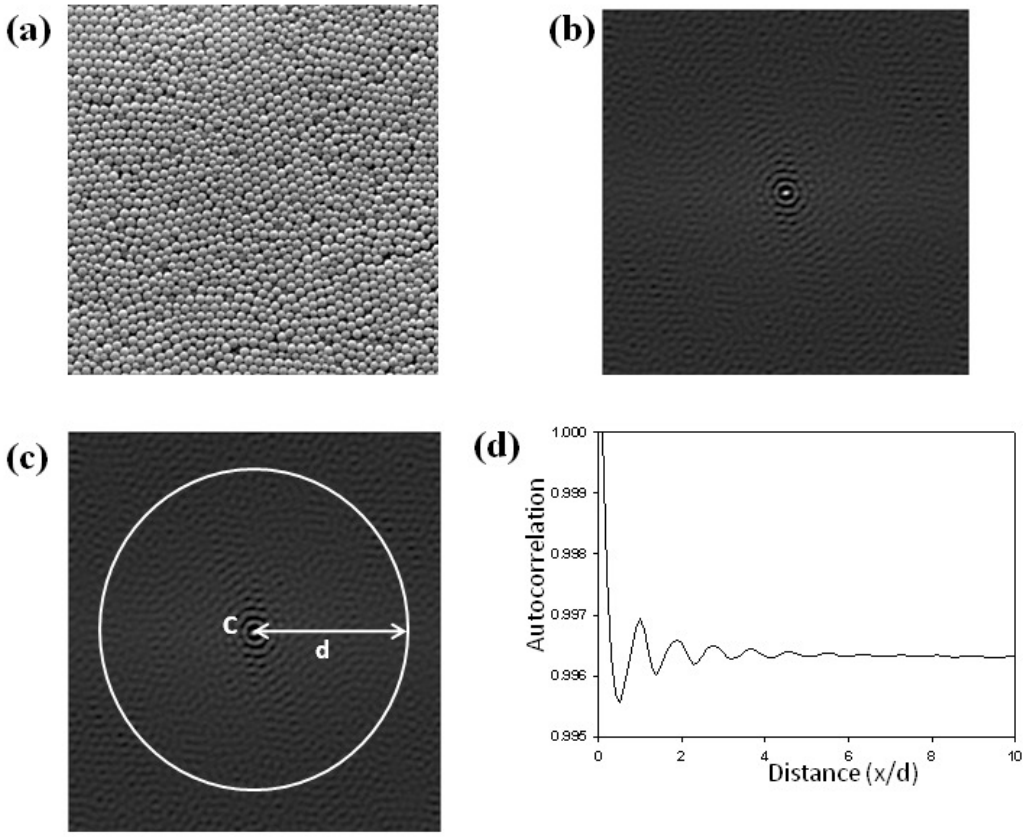

Figure 2.3. SEM image of colloidal amorphous (a), autocorrelation function obtained from the SEM image (b), the circular area which was considered to create radial profile plot (c) and the radial profile plot for M1, here, *x* and *d* on the horizontal axis are the distance from an arbitrary particle and the distance between the center of the circle (which was taken for calculating the radial profile) with any point on its circumference in pixels (d).

2.2.5. Digital Optical Microscopy

In order to check the viewing angle dependence of the structural colors of the prepared samples, photograph were taken on a digital microscope (KEYENCE VHX-500). The dried samples were kept on the stage under the microscopic lens and were illuminated by halogen light source (OLYMPUS LG-PS2). The objective lens was kept fixed at perpendicular to the surface plane of the sample whereas the incident angle of light was altered from 0^o to 40^o. The shutter speed of the lens was 1/15 sec and the numerical aperture (NA) was 0.82, during the capturing of images at each incident angle.

2.2.6. Spectroscopic Observation

The transmittance spectra of samples were measured using Ocean Optics USB2000 fiber optic spectrometer in methanol by altering the angle of incidence from 0^o to 40^o. The diffraction of light from colloidal aggregations of high refractive index contrast (i.e., the difference of the refractive index of the sphere portion relative to the gap portion), such as the air-filled SiO_2 colloidal array, is very strong, and the amplitude of the radiation attenuates rapidly as the propagation distance into the aggregations increases.[33] As a result, most of the incident light interacts only with about a dozen layers near the surface. Thus, experimentally obtained reflection spectra for the air-filled SiO_2 colloidal aggregations are reflected in the interactions in the vicinity of the surface, and are not reflected in the internal structure. One can control the dielectric contrast by filling the intersphere voids with dielectric fluids in order to identify the internal structure of the aggregations.[4] In this experiment, the intersphere voids of the colloidal crystal and the colloidal amorphous are impregnated with methanol that has refractive index (1.3292 at 20 °C for 589.3 nm) higher than that of

air (1.0003 at 15 °C for 589.3 nm). The experimentally obtained refractive index of the SiO_2 particles is about 1.39.[4] The smoothly varying background was subtracted from the spectra prior to further analysis because the characteristic spectrum domain corresponding to the appearance of color exhibited a shoulder shape in the unprocessed spectrum.

2.3. References

[1] Mayoral, R.; Requena, J.; Moya, J. S.; López, C.; Cintas, A.; Míguez, H.; Meseguer, F.; Vázquez, L.; Holgado, M.; Blanco, A. *Adv. Mater.* **1997**, *9*, 257−258.

[2] Jiang, P.; McFarland, M. J. *J. Am. Chem. Soc.* **2004**, *126*, 13778−13786.

[3] Van Blaaderen, A.; Ruel, R.; Wiltzius, P. *Nature***1997**, *385*, 321−324.

[4] Allard, M.; Sargent, E. H.; Lewis, P. C.; Kumacheva, E. *Adv. Mater.* **2004**, *16*, 1360−1364.

[5] Lu, Y.; Yin, Y.; Gates, B.; Xia, Y. *Langmuir***2001**, *17*, 6344−6350.

[6] Park, S. H.; Qin, D.; Xia, Y. *Adv. Mater.* **1998**, *10*, 1045−1049.

[7] Míguez, H.; Yang, S. M.; Ozin, G. A. *Appl. Phys. Lett.***2002**, *81*, 2493−2495.

[8] Kumacheva, E.; Golding, R. K.; Allard, M.; Sargent, E. H. *Adv. Mater.***2002**, *14*, 221−224.

[9] Vickreva, O.; Kalinina, O.; Kumacheva, E. *Adv. Mater.* **2000**, *12*, 110−112.

[10] Trau, M.; Saville, D. A.; Aksay, I. A. *Science***1996**, *272*, 706−709.

[11] Rogach, A. L.; Kotov, N. A.; Koktysh, D. S.; Ostrander, J. W.; Ragoisha, G. A. *Chem. Mater.* **2000**, *12*, 2721−2726.

[12] Helseth, L. E.; Wen, H. Z.; Hansen, R. W.; Johansen, T. H.; Heinig, P.; Fischer, T. M. *Langmuir***2004**, *20*, 7323−7332.

[13] Jiang, P.; Bertone, J. F.; Hwang, K. S.; Colvin, V. L. *Chem. Mater.* **1999**, *11*, 2132−2140.

[14] Denkok, N. D.; Velev, O. D.; Kralchevsky, P. A.; Ivanov, I. B.; Yoshimuri, H.; Nagayama, K. *Langmuir***1992**, *8*, 3183−3190.

[15] Cong, H.; Cao, W. *Langmuir***2003**, *19*, 8177−8181.

[16] Ye, Y.-H.; LeBlanc, F.; Hache, A.; Truong, V. V. *Appl. Phys. Lett.***2001**, *78*, 52−54.

[17] Rodner, S. C.; Wedin, P.; Bergström, L. *Langmuir***2002**, *18*, 9327−9333.

[18] McLachlan, M. A.; Johnson, N. P.; De La Rue, R. M.; McComb, D. W. *J. Mater. Chem.***2004**, *14*, 144−150.

[19] Dimitrov, A. S.; Nagayama, K. *Langmuir* **1996**, *12*, 1303−1311.

[20] Rengarajan, R.; Mittleman, D.; Rich, C.; Colvin, V. *Phys. Rev. E***2005**, *71*, 16615.

[21] Gates, B.; Xia, Y. *Appl. Phys. Lett*. **2001**, *78*, 3178−3180.

[22] Vlasov, A.; Kaliteevski, M. A.; Nikolaev, V. V. *Phys. Rev. B***1999**, *60*, 1555−1562.

[23] Li, Z.-Y.; Zhang, Z.-Q. *Phys. Rev. B***2000**, *62*, 1516−1519.

[24] Kaliteevski, M.; Manzanares Martinez, J.; Cassagne, D.; Albert, J. P. *Phys. Status Solidi* **2003**, *195*, 612−617.

[25] Allard, M.; Sargent, E. H.; Kumacheva, E.; Kalinina, O. *Opt. QuantumElectron.* **2002**, *34*, 27−36.

[26] Rojas-Ochoa, L. F.; Mendez-Alcaraz, J. M.; Sáenz, J. J.; Schurtenberger, P.; Scheffold, F. *Phys. Rev. Lett*, **2004**, *93*, 73903.

[27] Solovyev, V. G.; Romanov, S. G.; Chigrin, D. N.; Sotomayor Torres, C. M. *Synth. Met.* **2003**, *139,* 601−604.

[28] Ballato, J.; Dimaio, J.; James, A.; Gulliver, E. *Appl. Phys. Lett.* **1999**, *75*, 1497

[29] Kaliteevski, M. A.; Martinez, J. M.; Cassagne, D.; Albert, J. P. *Phys. Rev. B***2002**, *66,* 113101.

[30] Allard, M.; Sargent, E. H. *Appl. Phys. Lett*. **2004**, *85*, 5887−5889.

[31] R. O. Prum, R. H. Torres, *Integr. Comp. Biol.* 2003, *43*, 591-602.

[32] C. E. Ayres, B. S. Jha, H. Meredith, J. R. Bowman, G. L. Bowlin, S. C. Henderson, D. G. Simpson, *J. Biomater. Sci. Polymer Edn.* 2008, *19*, 603-621.

[33] J. F. Bertone, P. Jiang, K. S. Hwang, D. M. Mittleman, V. L. Colvin, *Phys. Rev. Lett.* 1999, *83*, 300-303.

[34] Y. Takeoka, T. Seki, *Langmuir* 2006, *22*, 10223-10232.

CHAPTER 3

RESULTS AND DISCUSSIONS

3.1. General

The purpose of this study is to prepare the source, which will exhibit structural color and the displayed color will be uniform at different viewing angle. On the basis of the hypothesis it was aimed to prepare some microstructure which will be different in nature from the view point of crystalline structure and will possess required optical properties. Here both types of microstructures such as crystalline microstructure (colloidal crystal) and amorphous microstructures were prepared in different methods. Then the morphology and the optical properties of all types of samples were characterized with the help of SEM, digital optical microscopy, optical spectroscopy and image processing techniques. Pictographic evidences along with spectrometric measurements validate that the structural color displayed by the amorphous system is independent of viewing angle and direction of incident light while the customized image analysis of scanning electron micrographs with valid theoretical explanation clarify the authentication of angle independence.

3.2. Crystalline Micro-structure

Throughout this study, colloidal crystal (CC) has been taken as a representative of crystalline micro-structure. The colloidal array, prepared by simple evaporation method consists of only 310 nm silica colloidal particles, is organized into a close-packed arrangement with a long-range order (hereinafter called “colloidal crystal”). The morphology and the optical properties of CC have been studied in order to compare with those of the amorphous micro-structures (AM).

3.2.1. Morphology Study

CC was prepared through the above described procedure and obtained their surface structures through Scanning Electron Microscopy (SEM). Highly ordered three-dimensional structure is visible in SEM image. Hexagonal close packed with a long-range ordered structure can be confirmed from the SEM image.

Scanning Electron Microscopy is one of the most practicable methods to elucidate the particle arrangement of colloidal array samples. Using SEM combined with image processing technique such as two-dimensional (2D) Fast Fourier Transform (FFT) operation, we established an independent measure of the ordering of our samples. The conversion of spatial information in the SEM image into a mathematically defined frequency domain or power spectrum pattern can be obtained from 2D FFT operation. This characteristic power spectrum pattern or frequency domain called streak, depicts the rate at which pixel intensities change in the spatial domain. For 2D FFT analysis the SEM images were converted into power of 2 (such as 256X256, 512X512 etc). In 2D FFT operation, the pattern of the distribution of grayscale pixels is used to estimate the arrangement of particles in crystal structure and amorphous structure. When a data image containing a long-range order of arranged particles is processed by 2D FFT, the resulting frequency plot contains pixels that are aligned along specific axis.

Therefore, a resulting frequency plot containing pixels aligned along an axis was obtained in the case of colloidal crystal. The hexagonal sharp peaks in the 2D FFT (Figure 3.1(b)) of the SEM image confirm the presence of long-range crystalline order.

The autocorrelation function represents the interrelationship of the contrast function, and thereby providing a measure of the translational symmetry in the system.

If the particles are organized with a regular distance between first neighbors, the autocorrelation function presents a maximum at the corresponding distance. Accordingly, the autocorrelation function for the system, which does not have any particular oriented structure, is a delta or decaying function. The array images taken by SEM were subjected to some image processing techniques that were designed to check the presence of long-range or short-range order in samples. The radial profile plot (Figure 3.1(c)) corresponding to the colloidal crystal contains a periodic distribution of maxima along an extended distance. Such distribution of maxima depict that the particles in the colloidal crystal are arranged in a periodic order and the repetition of such periodic order prevail all over the colloidal crystal's structure.

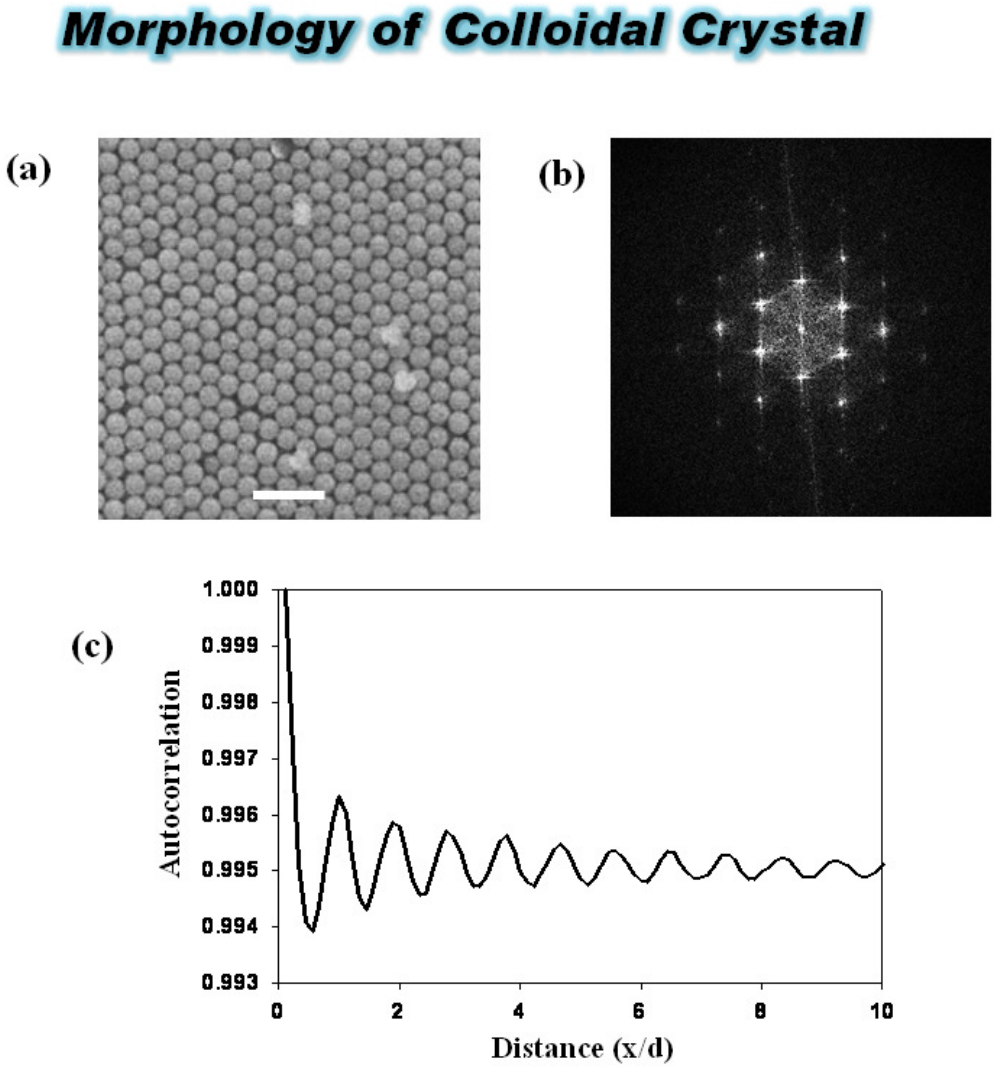

Figure 3.1. SEM image of colloidal crystal (a), 2D FFT (b) and the radial profile plot of colloidal crystal calculated from autocorrelation function (c). Scale bar is 1 μm.

3.2.2. Digital Optical Microscopic Observation

The structural color (Figure 3.2 (a)) displayed by colloidal crystal is angle dependent:[1] the colloidal crystal's structural color shifts when the angle of view or the angle of illumination or both is altered. Figure evidences the angle dependence optical images of the structural color of the colloidal crystal obtained. The observable structural color in viewing angle direction is considerably different from at 0 ^{o}: the structural color changed from red to green when the angle of illumination was altered from 0 ^{o} to 40 ^{o}. The blue shift of the reflection can be observed due to the Bragg diffraction of visible light from the ordered spheres. The structural color changes from red to green.

3.2.3. Optical Spectroscopic Measurement

Figure 3.2 (b) shows representative optical transmission spectra measured for the colloidal crystal, which were immersed in methanol. The diffraction of light from colloidal aggregations of high refractive index contrast (i.e., the difference of the refractive index of the sphere portion relative to the gap portion), such as the air-filled SiO_2 colloidal array, is very strong, and the amplitude of the radiation attenuates rapidly as the propagation distance into the aggregations increases.[2] As a result, most of the incident light interacts only with about a dozen layers near the surface. Thus, experimentally obtained reflection spectra for the air-filled SiO_2 colloidal aggregations are reflected in the interactions in the vicinity of the surface, and are not reflected in the internal structure. One can control the dielectric contrast by filling the intersphere voids with dielectric fluids in order to identify the internal structure of the aggregations.[3] In this experiment, the intersphere voids of the colloidal crystal and the colloidal amorphous are impregnated with methanol that has refractive index

(1.3292 at 20 °C for 589.3 nm) higher than that of air (1.0003 at 15 °C for 589.3 nm). The experimentally obtained refractive index of the SiO_2 particles is about 1.39.[3]

The smoothly varying background was subtracted from the spectra prior to further analysis because the characteristic spectrum domain corresponding to the appearance of color exhibited a shoulder shape in the unprocessed spectrum. In the case of the colloidal amorphous comparatively broad peaks were observed in transmittance spectra whereas sharp and clear peaks which, however, is not complete photonic band gap were observed for the colloidal crystal: these are so-called pseudo-gaps with prominent depletions of the photonic densities of states. Wavelength of the reflected color from the colloidal crystal becomes shorter as viewing angle becomes greater. Such shift observed from the colloidal crystal is explained by Bragg scattering of photons due to the periodical dielectric structure.

For CC the peak position shifts from 690 nm to 650 nm wavelength.

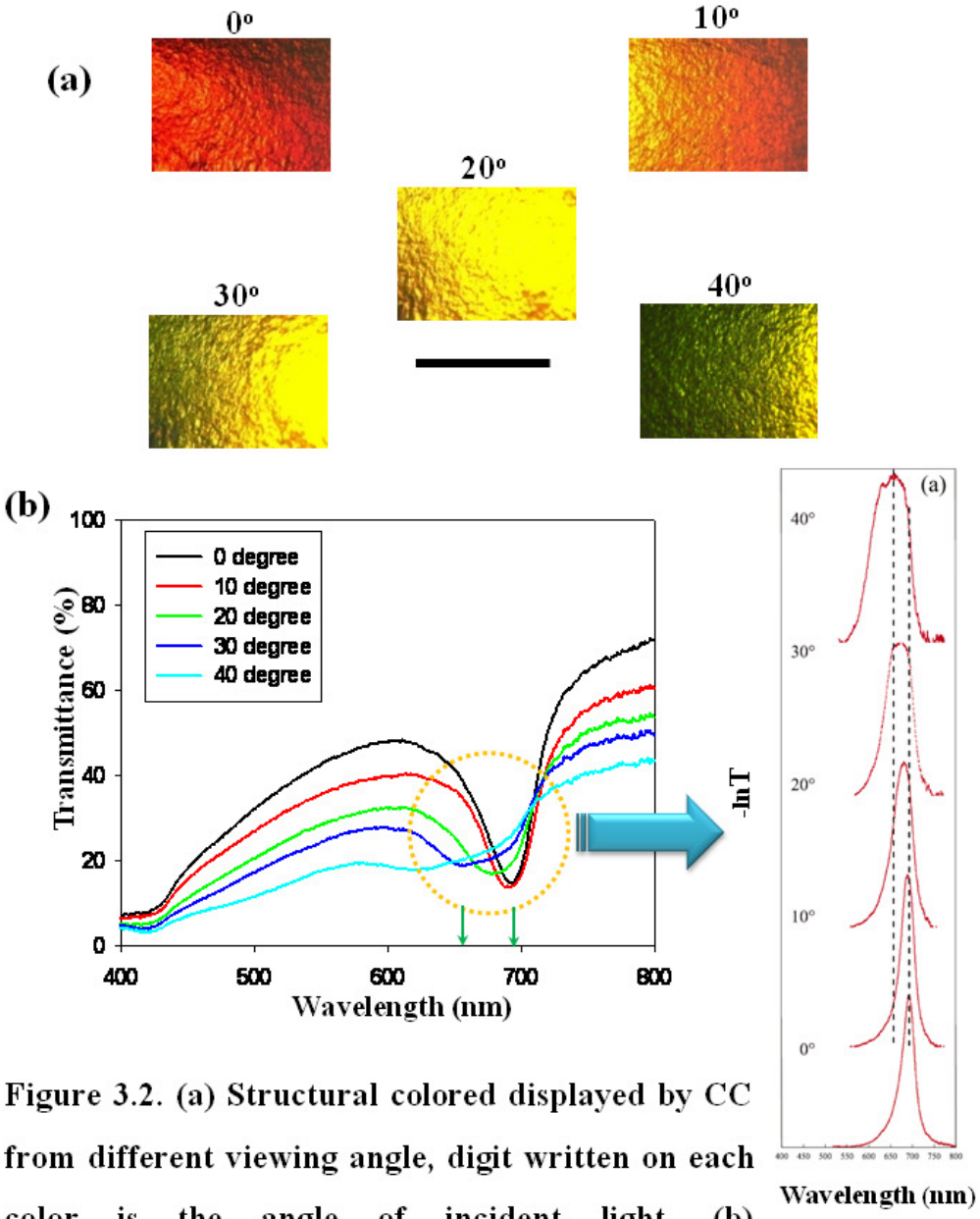

Figure 3.2. (a) Structural colored displayed by CC from different viewing angle, digit written on each color is the angle of incident light. (b) Transmittance spectra of CC under methanol. The scale bar is 1 mm.

3.3. Amorphous Micro-structures

Five samples were prepared by mixing two different sized silica colloidal particles having the diameter of 310 nm and 220 nm with the same method consist of roughly packed silica spheres (hereinafter called “amorphous microstructure”). Silica colloidal particles having the diameter of 310 nm were used as host and 220 nm sized silica colloidal particles were taken as guest. So here the addition of the smaller particles to the larger particles is termed as doping. Thus by changing the doping concentration five samples of amorphous microstructure were prepared. Doping concentration was varied from 10 wt. % to 50 wt. %. Fabricated samples were tagged as M1 (310 nm- 90 wt. % and 220 nm- 10 wt. %), M2 (310 nm- 80 wt. % and 220 nm- 20 wt. %), M3 (310 nm- 70 wt. % and 220 nm- 30 wt. %), M4 (310 nm- 60 wt. % and 220 nm- 40 wt. %) and M5 (310 nm- 50 wt. % and 220 nm- 50 wt. %).

3.3.1. Amorphous Micro-structures M1

3.3.1.1. Morphology Study

In amorphous microstructure M1 contains 90 wt. % of silica colloidal particle of 310 nm diameter and 10 wt. % of silica colloidal particle of 220 nm diameter. Surface structure was obtained through Scanning Electron Microscopy (SEM). SEM images of the colloidal amorphous have been shown in Figure 3.3 (a) as examples of the part of the exposed surfaces of the colloidal amorphous samples. The presence of size variation in the colloidal suspension influences the colloidal particles to be arranged in a disordered state.[4] Particle orientation varies from fragment to fragment. The different structural arrangements seem to be related to variations of the weight proportions of the two sizes of sphere in different places. Some places contained

disordered mixtures of the two sizes, and in some places there are boundaries across which small spheres appeared to have penetrated into an array of larger ones. The possibilities for the occurrence of long-range order in the arrangement of particle decrease as the proportion of the smaller colloidal particles increases.

The SEM images of the samples consisting of two particles with different size were subjected to 2D FFT operation in order to track and map these particle distributions over the surfaces. Frequency plots (figure 3.3 (b)) containing clusters of white pixels, which are intensified in symmetrical and circular patterns around the origin, were found. The discrete rings in 2D FFT of the images indicate that the periodicity of spatial variation in refractive index is equivalent in all directions in these planes within the samples: these SiO_2 colloidal particles form amorphous arrays with local and spatially isotropic structural correlation. In the case of M1, radial profile plot (figure 3.3 (c)) shows distinct features that vary from CC. The repetition of the periodic distribution of maxima for M1 appears several times but less than that of the colloidal crystal. The lacking of crystalline periodicity becomes larger when the amount of 220 nm SiO_2 particle increases.

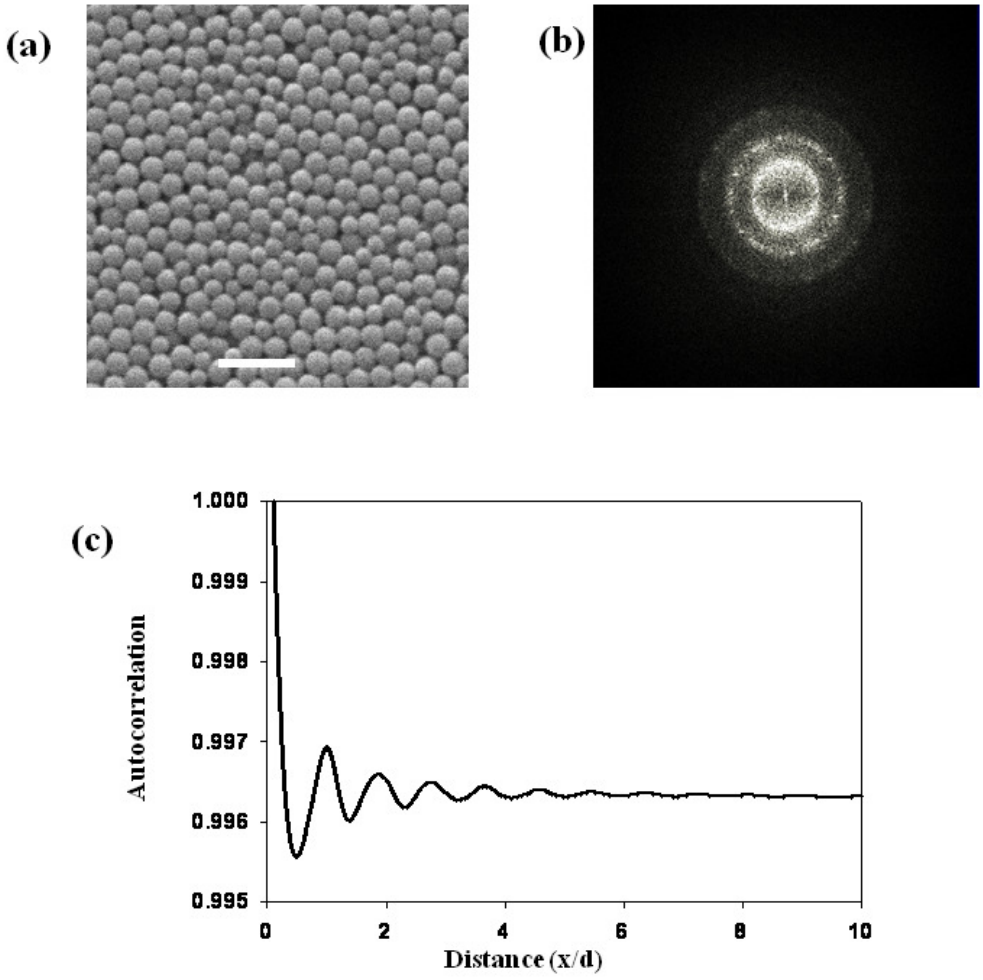

Figure 3.3. SEM image of M1 (a), 2D FFT (b) and the radial profile plot of M1 calculated from autocorrelation function (c). Scale bar is 1 μm.

3.3.1.2. Digital Optical Microscopic Observation

The colloidal amorphous, M1, exhibits somewhat pink structural color that remains constant during the change of the angle of illumination. Color shift from 0^o up to 40^o in viewing angle is unambiguously quite lower or almost negligible, compared to the case of the colloidal crystal.

3.3.1.3. Optical Spectroscopic Measurement

In the case of M1comparatively broad peaks were observed in transmittance spectra. The occurrence of the broadening of the width of the peak for the colloidal amorphous must be influenced by disorder. However, the peak positions in the transmittance spectra of the colloidal amorphous arrays are virtually angle independent. We plotted the peak positions of the transmittance spectra for the colloidal crystal and the colloidal amorphous arrays against the corresponding angle of illumination in Figure. They show an adequately good verification for the influence of viewing angle on the structural color exhibited by the colloidal amorphous, M1. When the angle of illumination was altered the positions of peaks shifted accordingly for the colloidal crystal but the positions of peaks for the colloidal amorphous were almost unchanged. For M1 the peak position changes at the very vicinity of 660 nm wavelength.

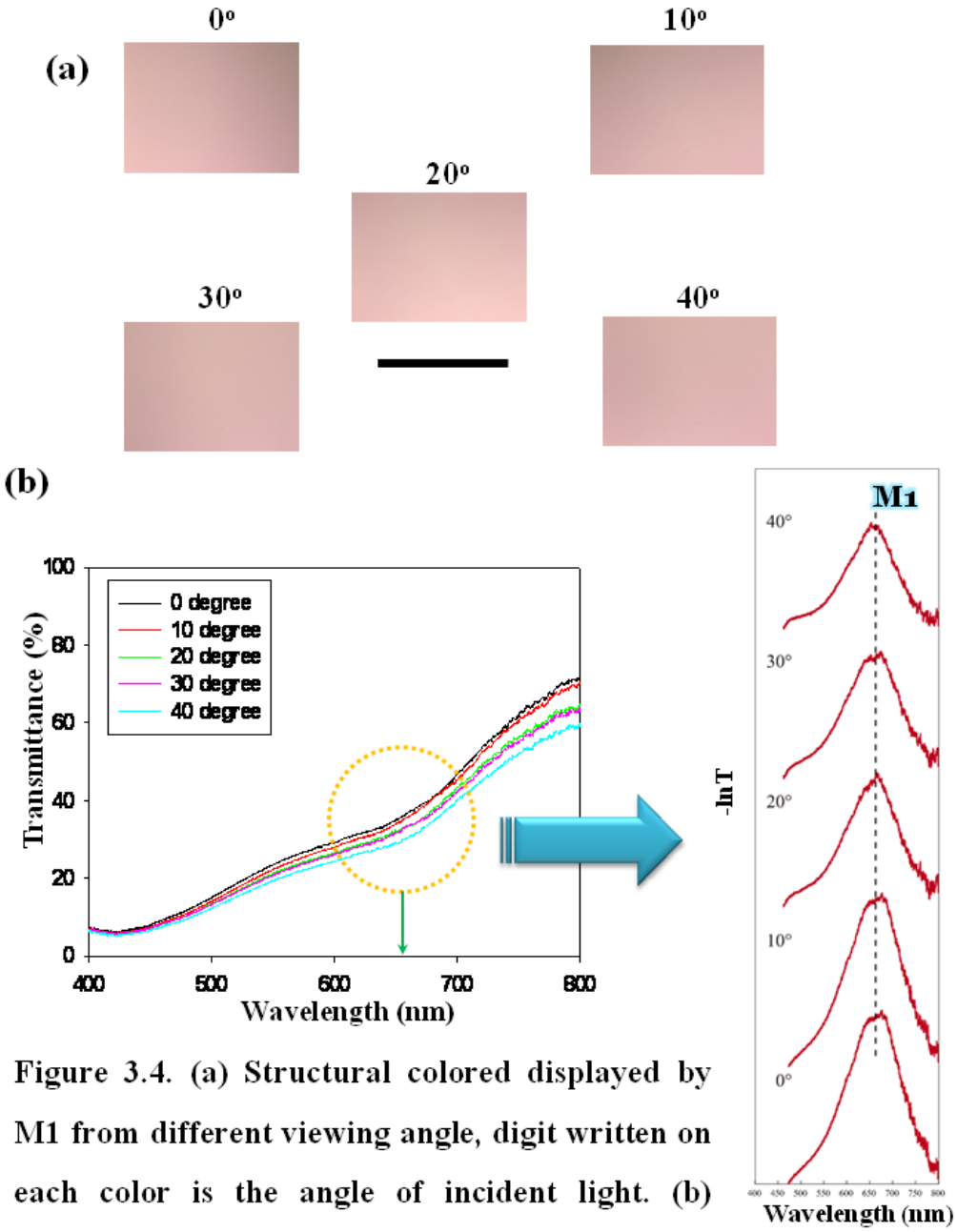

Figure 3.4. (a) Structural colored displayed by M1 from different viewing angle, digit written on each color is the angle of incident light. (b) Transmittance spectra of M1 under methanol. The scale bar is 1 mm.

3.3.2. Amorphous Micro-structures M2

3.3.2.1. Morphology Study

In amorphous microstructure M2 contains 80 wt. % of silica colloidal particle of 310 nm diameter and 20 wt. % of silica colloidal particle of 220 nm diameter. The presence of size variation in the colloidal suspension influences the colloidal particles to be arranged in a disordered state.[4] Particle orientation varies from fragment to fragment. The different structural arrangements seem to be related to variations of the weight proportions of the two sizes of sphere in different places. The possibilities for the occurrence of long-range order in the arrangement of particle decrease as the proportion of the smaller colloidal particles increases. As a result the occurrences of long-range order in M2 are fewer than that of M1.

In the case of M2, radial profile plots show distinct features that vary from CC as well as M1. The repetition of the periodic distribution of maxima for M2 appears several times but less than that of the colloidal crystal and M1. The lacking of crystalline periodicity becomes larger when the amount of 220 nm SiO_2 particle increases.

In figure 3.5, the morphology of M2 has been shown.

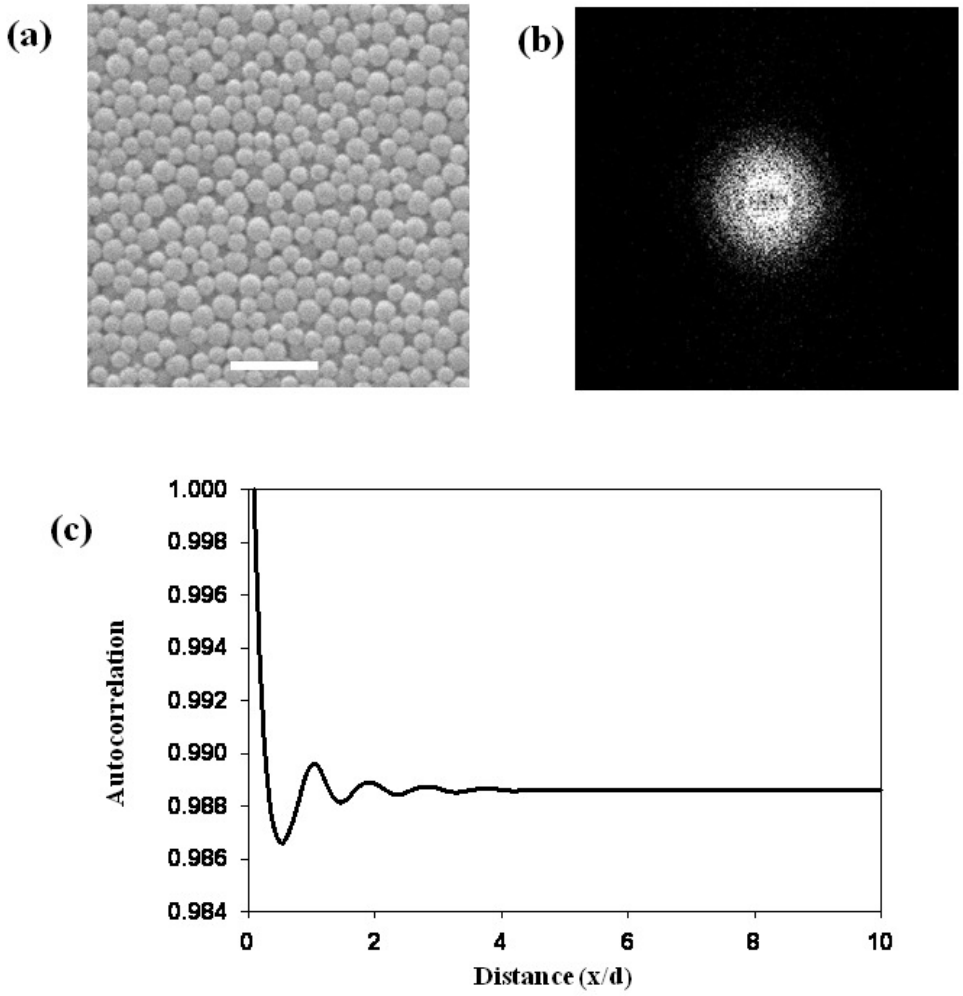

Figure 3.5. SEM image of M2 (a), 2D FFT (b) and the radial profile plot of M2 calculated from autocorrelation function (c). Scale bar is 1 μm.

3.3.2.2. Digital Optical Microscopic Observation

M2 exhibits red-orange structural color (figure 3.6 (a)) that remains constant during the change of the angle of illumination. Color shift from 0^o up to 40^o in viewing angle is unambiguously quite lower or almost negligible, compared to the case of the colloidal crystal.

3.3.2.3. Optical Spectroscopic Measurement

In the case of M2 comparatively broad peaks were observed in transmittance spectra. When the angle of illumination was altered the positions of peaks shifted accordingly for the colloidal crystal but the positions of peaks for M2 were almost unchanged (figure 3.6 (b)). For M2 the peak position changes at the very vicinity of 640 nm wavelength.

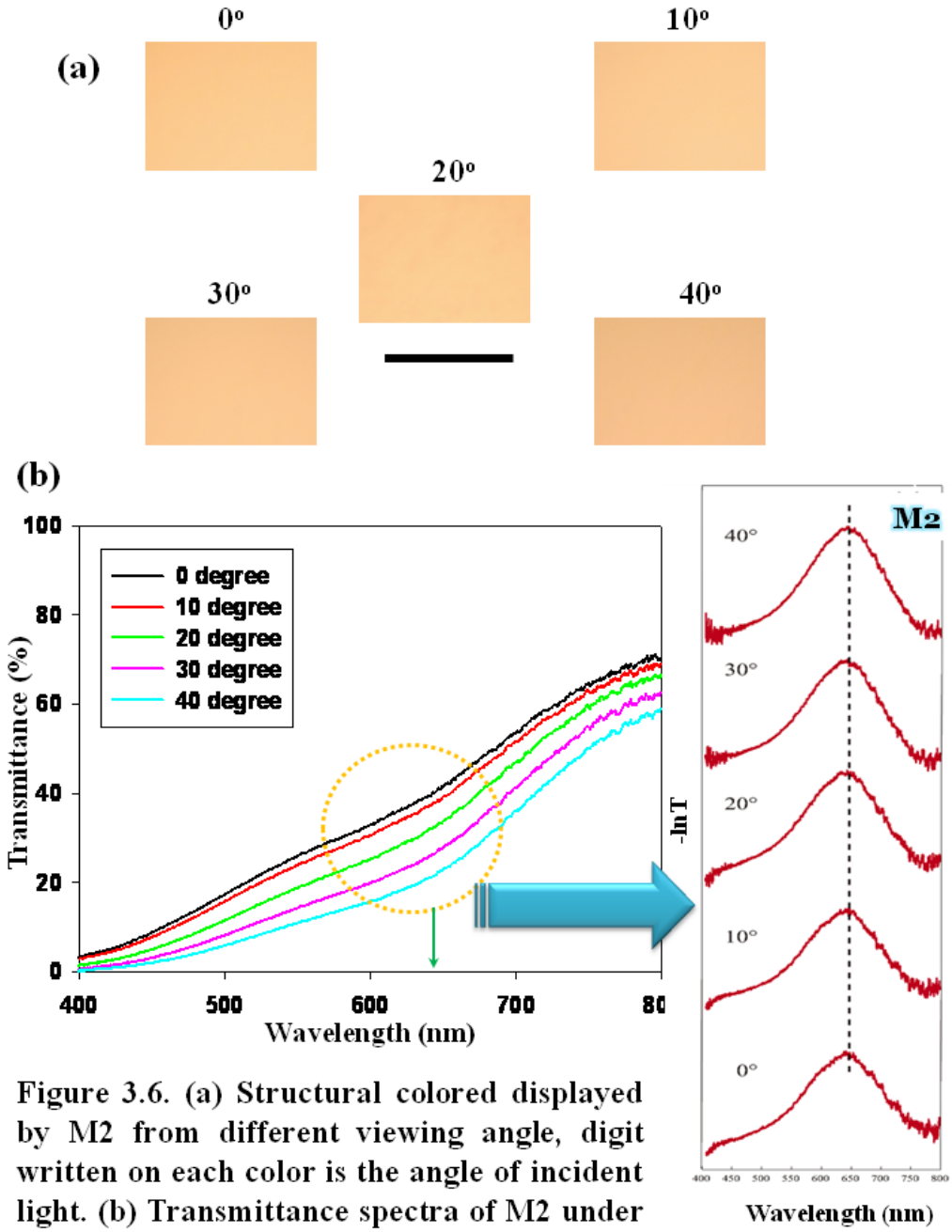

Figure 3.6. (a) Structural colored displayed by M2 from different viewing angle, digit written on each color is the angle of incident light. (b) Transmittance spectra of M2 under methanol. The scale bar is 1 mm.

3.3.3. Amorphous Micro-structures M3

3.3.3.1. Morphology Study

In amorphous microstructure M3 contains 70 wt. % of silica colloidal particle of 310 nm diameter and 30 wt. % of silica colloidal particle of 220 nm diameter. The presence of size variation in the colloidal suspension influences the colloidal particles to be arranged in a disordered state.[4] Particle orientation varies from fragment to fragment. The different structural arrangements seem to be related to variations of the weight proportions of the two sizes of sphere in different places. The possibilities for the occurrence of long-range order in the arrangement of particle decrease as the proportion of the smaller colloidal particles increases. As a result the occurrences of long-range order in M3 are fewer than that of M1 and M2.

In the case of M3, radial profile plots show distinct features that vary from M1 as well as M2. The repetition of the periodic distribution of maxima for M3 appears several times but less than that of M2 and M1. The lacking of crystalline periodicity becomes larger when the amount of 220 nm SiO_2 particle increases.

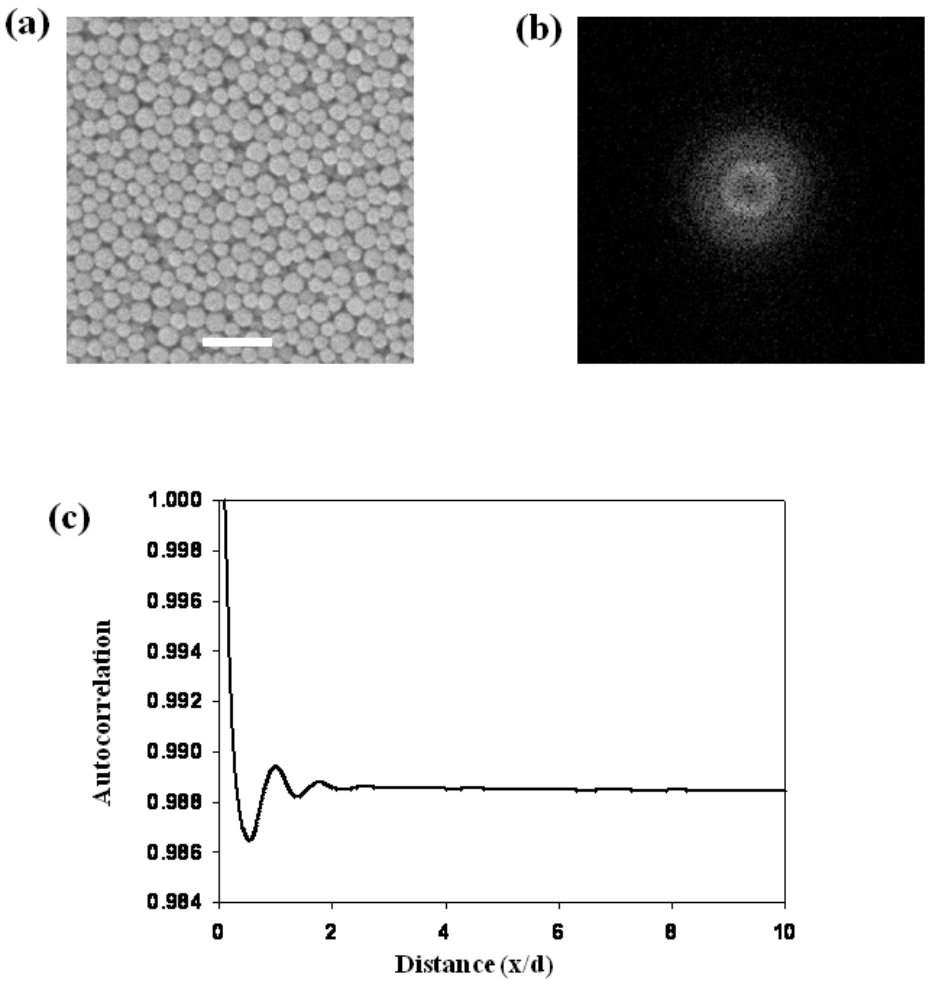

Figure 3.7. SEM image of M3 (a), 2D FFT (b) and the radial profile plot of M3 calculated from autocorrelation function (c). Scale bar is 1 μm.

3.3.3.2. Digital Optical Microscopic Observation

M3 exhibits orange structural color that remains constant during the change of the angle of illumination. Color shift from 0^o up to 40^o in viewing angle is unambiguously quite lower or almost negligible, compared to the case of the colloidal crystal.

3.3.3.3. Optical Spectroscopic Measurement

In the case of M3 comparatively broad peaks were observed in transmittance spectra. When the angle of illumination was altered the positions of peaks shifted accordingly for the colloidal crystal but the positions of peaks for M3 were almost unchanged. For M3 the peak position changes at the very vicinity of 625 nm wavelength.

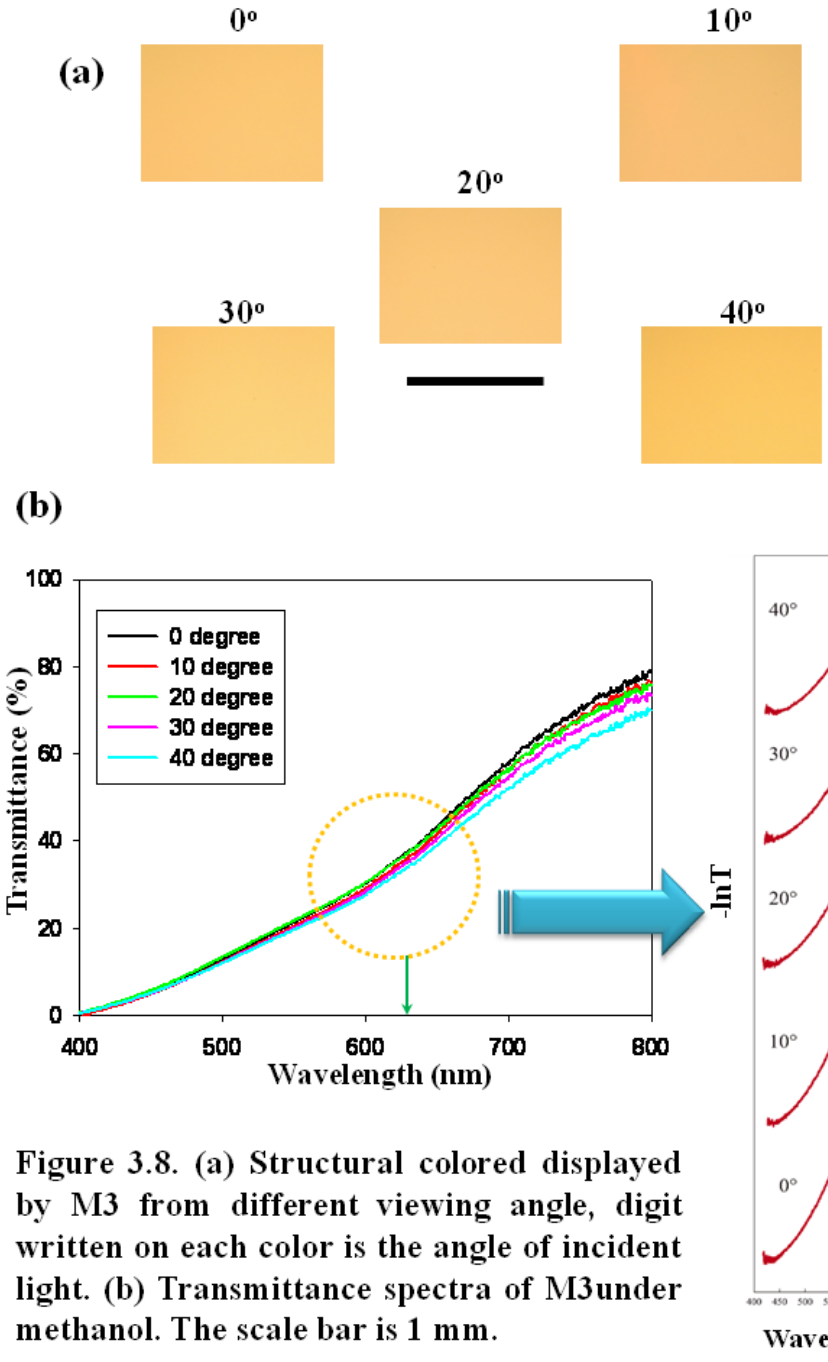

Figure 3.8. (a) Structural colored displayed by M3 from different viewing angle, digit written on each color is the angle of incident light. (b) Transmittance spectra of M3under methanol. The scale bar is 1 mm.

3.3.4. Amorphous Micro-structures M4

3.3.4.1. Morphology Study

In amorphous microstructure M4 contains 60 wt. % of silica colloidal particle of 310 nm diameter and 40 wt. % of silica colloidal particle of 220 nm diameter. The presence of size variation in the colloidal suspension influences the colloidal particles to be arranged in a disordered state.[4] Particle orientation varies from fragment to fragment. The different structural arrangements seem to be related to variations of the weight proportions of the two sizes of sphere in different places. The possibilities for the occurrence of long-range order in the arrangement of particle decrease as the proportion of the smaller colloidal particles increases. As a result the occurrences of long-range order in M4 are fewer than that of M1, M2 and M3.

In the case of M4, radial profile plots show distinct features that vary from M1, M2 and M3. The repetition of the periodic distribution of maxima for M4 appears several times but less than that of M1, M2 and M3. The lacking of crystalline periodicity becomes larger when the amount of 220 nm SiO_2 particle increases.

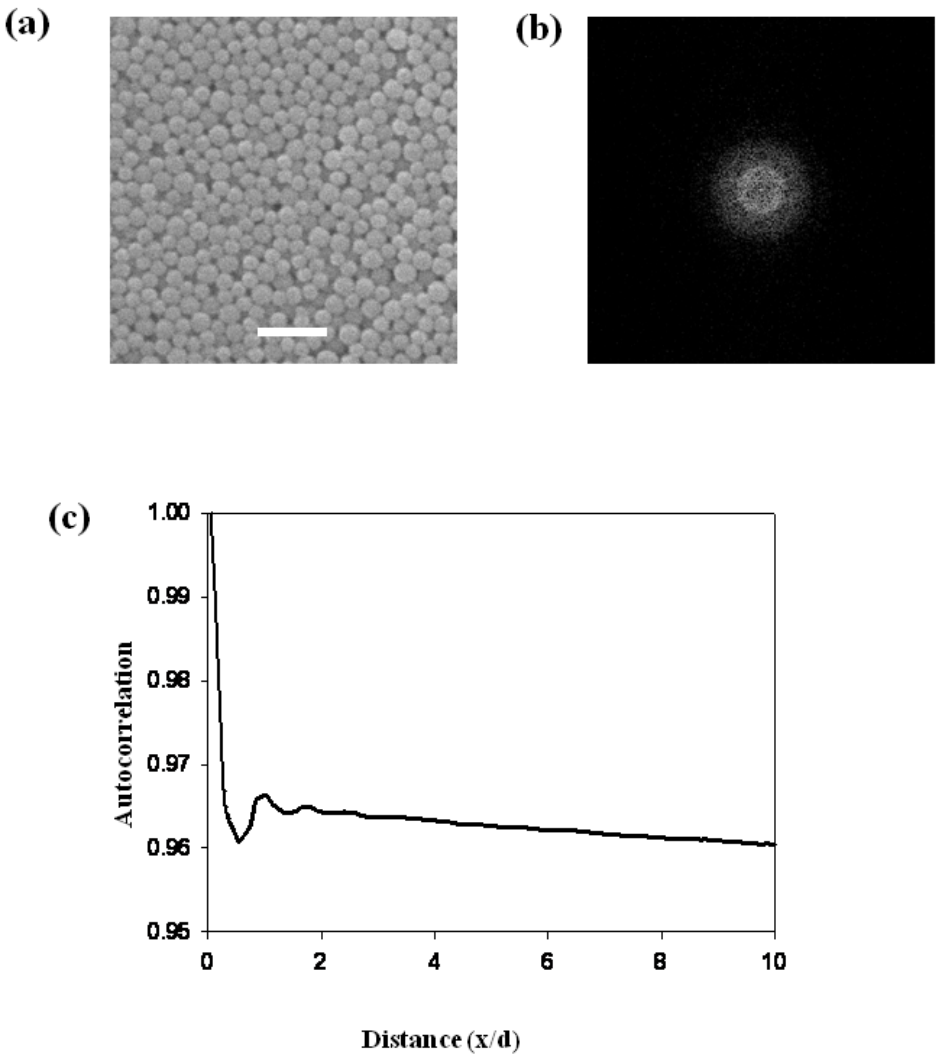

Figure 3.9. SEM image of M4 (a), 2D FFT (b) and the radial profile plot of M4 calculated from autocorrelation function (c). Scale bar is 1 μm.

3.3.4.2. Digital Optical Microscopic Observation

M4 exhibits yellow structural color that remains constant during the change of the angle of illumination. Color shift from 0^o up to 40^o in viewing angle is unambiguously quite lower or almost negligible, compared to the case of the colloidal crystal.

3.3.4.3. Optical Spectroscopic Measurement

In the case of M4 comparatively broad peaks were observed in transmittance spectra. When the angle of illumination was altered the positions of peaks shifted accordingly for the colloidal crystal but the positions of peaks for M4 were almost unchanged. For M4 the peak position changes at the very vicinity of 590 nm wavelength.

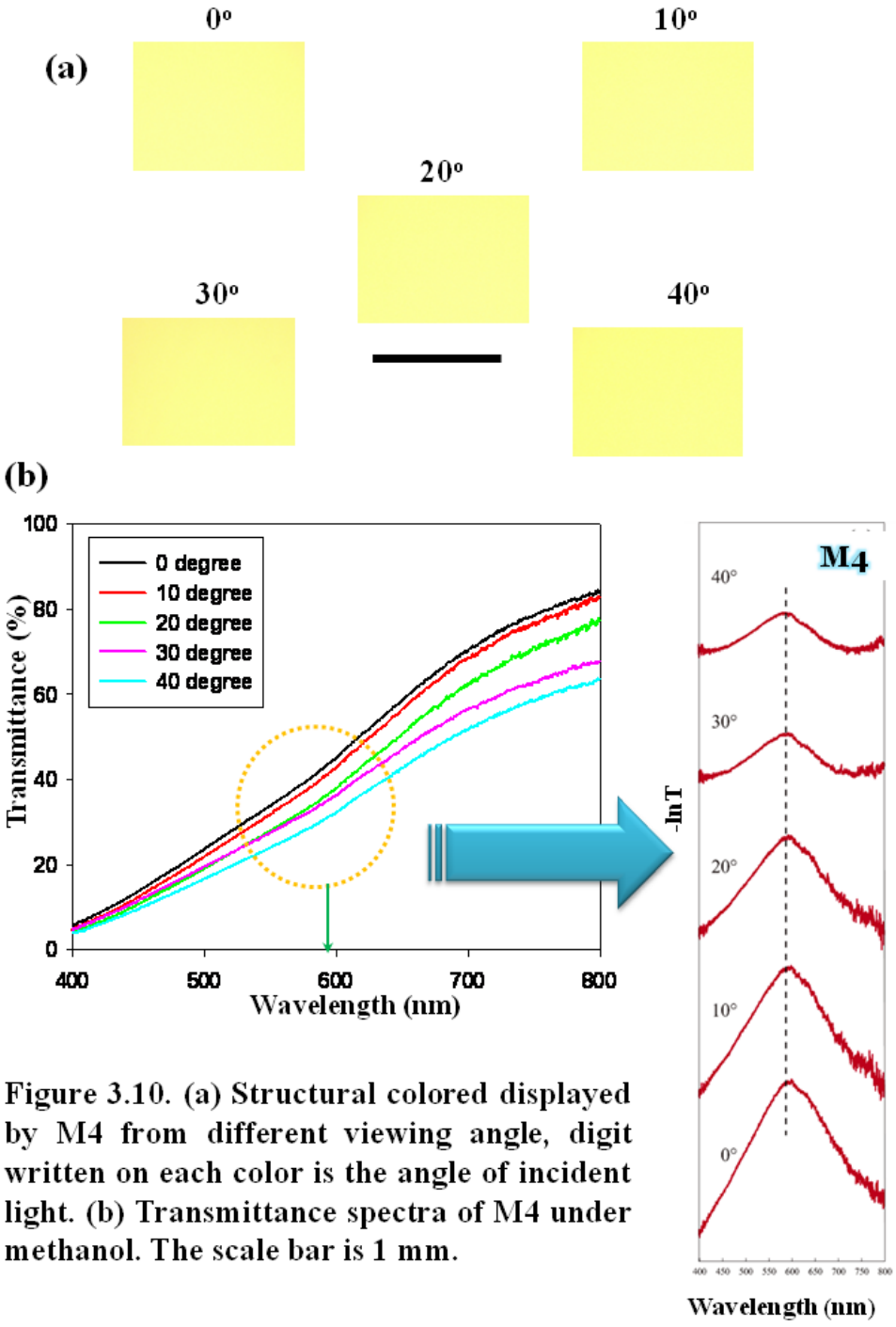

Figure 3.10. (a) Structural colored displayed by M4 from different viewing angle, digit written on each color is the angle of incident light. (b) Transmittance spectra of M4 under methanol. The scale bar is 1 mm.

3.3.5. Amorphous Micro-structures M5

3.3.5.1. Morphology Study

In amorphous microstructure M5 contains 50 wt. % of silica colloidal particle of 310 nm diameter and 50 wt. % of silica colloidal particle of 220 nm diameter. The presence of size variation in the colloidal suspension influences the colloidal particles to be arranged in a disordered state.[4] Particle orientation varies from fragment to fragment. The different structural arrangements seem to be related to variations of the weight proportions of the two sizes of sphere in different places. The possibilities for the occurrence of long-range order in the arrangement of particle decrease as the proportion of the smaller colloidal particles increases. As a result the occurrences of long-range order in M5 are fewer than that of M1, M2 and M3.

In the case of M5, radial profile plots show distinct features that vary from M1, M2 and M3. The repetition of the periodic distribution of maxima for M5 appears several times but less than that of M1, M2 and M3. The lacking of crystalline periodicity becomes larger when the amount of 220 nm SiO_2 particle increases.

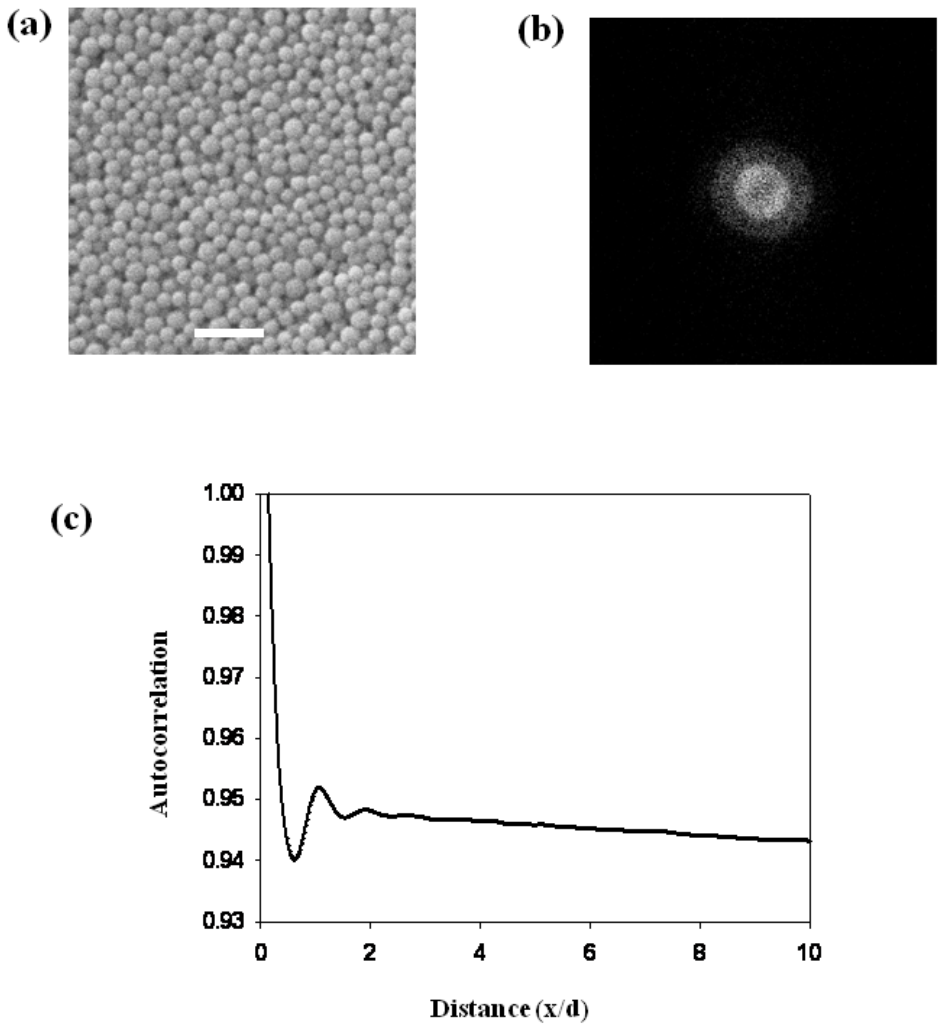

Figure 3.11. SEM image of M5 (a), 2D FFT (b) and the radial profile plot of M5 calculated from autocorrelation function (c). Scale bar is 1 μm.

3.3.5.2. Digital Optical Microscopic Observation

M5 exhibits greenish structural color that remains constant during the change of the angle of illumination. Color shift from 0^o up to 40^o in viewing angle is unambiguously quite lower or almost negligible, compared to the case of the colloidal crystal.

3.3.5.3. Optical Spectroscopic Measurement

In the case of M5 comparatively broad peaks were observed in transmittance spectra. When the angle of illumination was altered the positions of peaks shifted accordingly for the colloidal crystal but the positions of peaks for M5 were almost unchanged. For M5 the peak position changes at the very vicinity of 565 nm wavelength.

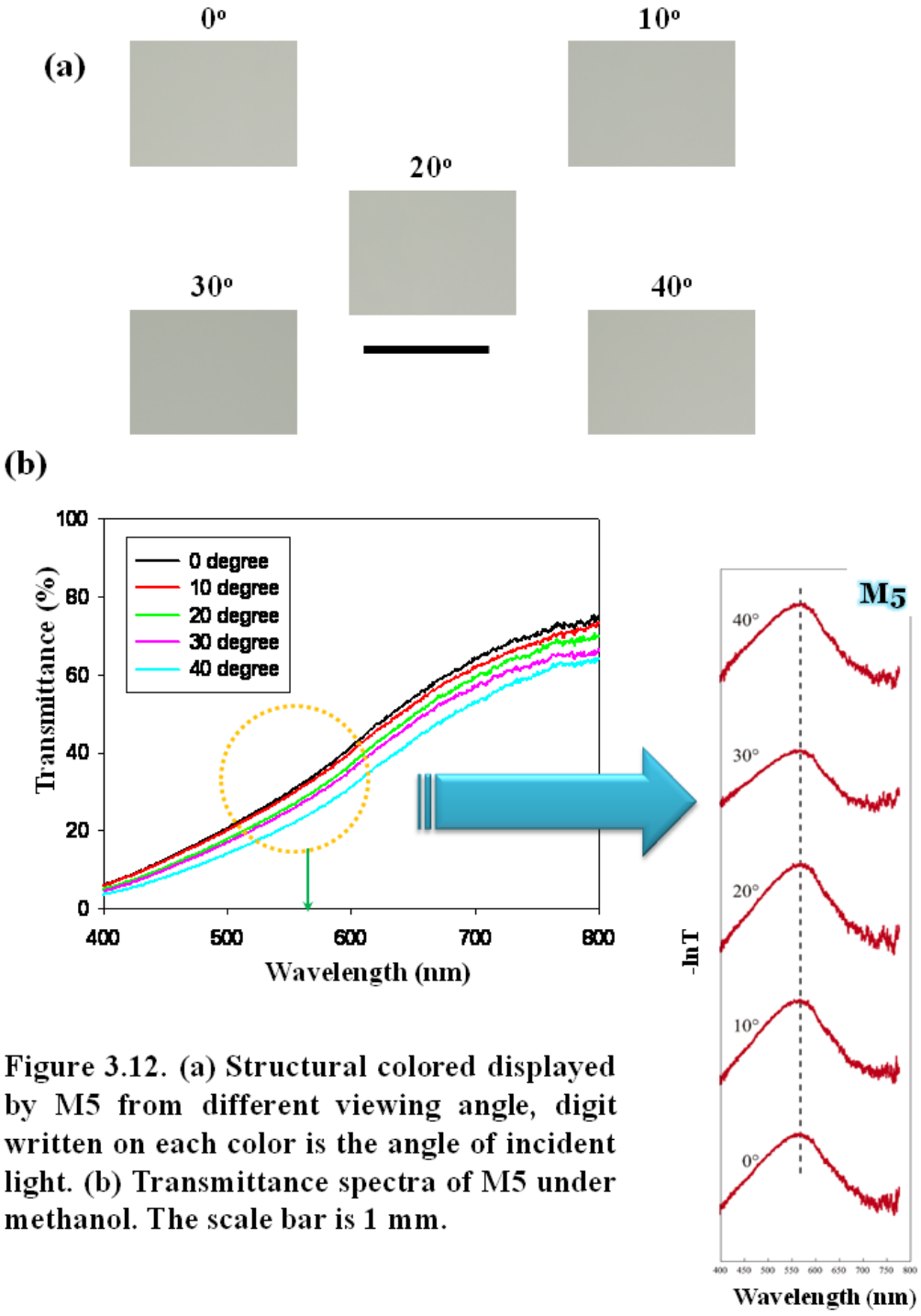

Figure 3.12. (a) Structural colored displayed by M5 from different viewing angle, digit written on each color is the angle of incident light. (b) Transmittance spectra of M5 under methanol. The scale bar is 1 mm.

3.4. Results and Discussions

In this study, we employ amorphous particle arrays consisting of two different submicron-sized monodispersed spherical silica particles to obtain structural colored materials without angle dependence, which is similar to an amorphous array of β-keratin particles in avian feather barbs. The amorphous arrays obtained reveal angle-independent matte structural colors depending on the weight ratio of the two differently sized silica particles. A pseudo-gap can be observed from the measurement of the transmission spectra of these samples. The peak positions of the pseudo-gap are virtually constant over incident angles between 0° and 40°.

The presence of size variation in the colloidal suspension causes the colloidal particles to be arranged in a disordered state. Particle orientation varies from fragment to fragment. The different structural arrangements seem to be related to variations in the weight proportions of the two sizes of spheres located in different places.

Using SEM combined with image processing techniques, such as two-dimensional (2D) fast Fourier transform (FFT), we established an independent measure of the ordering of our samples. In the case of the colloidal crystal, the resulting frequency plot contains pixels that are concentrated along a specific axis. The hexagonal sharp peaks in the 2D FFT of the SEM image confirm the presence of long-range crystalline order. On the other hand, frequency plots or power spectra contain clusters of white pixels that are concentrated in symmetrical, circular patterns around the origin, were found for SEM images of amorphous arrays. The discrete rings in the 2D FFTs of the images indicate that the periodicity of the spatial variation in the refractive index is equivalent in all directions in these planes within the samples; these SiO_2 colloidal particles form amorphous arrays with local and spatially isotropic

structural correlation. The array images taken by SEM were subjected to some image processing techniques that were designed to verify the presence of long-range or short-range order in the samples. The radial profile plot corresponding to the colloidal crystal contains a periodic distribution of maxima along an extended distance. Such distribution of the maxima indicates that the particles in the colloidal crystal are arranged in a periodic order and that the repetition of such periodic order is found throughout the colloidal crystal's structure. In the case of the mixed particle arrays, radial profile plots show distinct features that vary from one sample to another. The repetition of the periodic distribution of maxima for M1 appears several times but less often than that of the colloidal crystal. The lack of crystalline periodicity becomes more apparent when the amount of 220-nm SiO_2 particles increases. This is why the maxima appear less frequently in the radial profile plot for M3 than in that of M1. As described above, we succeeded in making amorphous particle arrays with short-range spatial order without having long-range order and periodicity, simply by mixing smaller-sized particles. This class of nanostructure is spatially isotropic and the composition varies identically in all direction with respect to the size of the wavelength.

The structural color displayed by the colloidal crystal is angle dependent; the colloidal crystal's structural color shifts when the angle of view, the angle of illumination, or both is altered. By contrast, the colloidal amorphous array displayed the same matte structural color although the angle of illumination was altered. The colloidal amorphous array M1 exhibited a somewhat pink structural color that remained constant with changes in the angle of illumination. The color shift from a 0^o to 40^o viewing angle was unambiguously lower or almost negligible compared with that of the colloidal crystal. Additionally, we found that simply varying the mixing

ratio of the two different particles controlled the hue of the angle-independent structural color.

The smoothly varying background was subtracted from the spectra prior to further analysis because the characteristic spectrum domain corresponding to the appearance of color exhibited a shoulder shape in the unprocessed spectrum. In the case of the colloidal amorphous array, comparatively broad peaks were observed in the transmittance spectra, whereas sharp and clear peaks, not corresponding to a complete photonic band gap, were observed for the colloidal crystal. These are so-called pseudo-gaps with prominent depletions of the photonic densities of states. The broadening of the width of the peak for the colloidal amorphous array must be influenced by disorder. The wavelength of the reflected color from the colloidal crystal becomes shorter as the viewing angle becomes greater. Such a shift was observed from the colloidal crystal and is explained by Bragg scattering of photons due to the periodical dielectric structure. However, the peak positions in the transmittance spectra of the colloidal amorphous arrays were virtually angle independent. We plotted the peak positions of the transmittance spectra for the colloidal crystal and the colloidal amorphous arrays against the corresponding angles of illumination. These plots (figure 3.13 (a)) provide verification of the influence of viewing angle on the structural color exhibited by the colloidal crystal and the colloidal amorphous array. Furthermore, we discovered that the peak wavelength became shorter as the content of smaller particles increased (figure 3.13 (b)). The systematic change in color seen in the optical images and transmission spectra of the colloidal amorphous arrays must be due to the change in the local correlation distance with varying particle composition.[5]

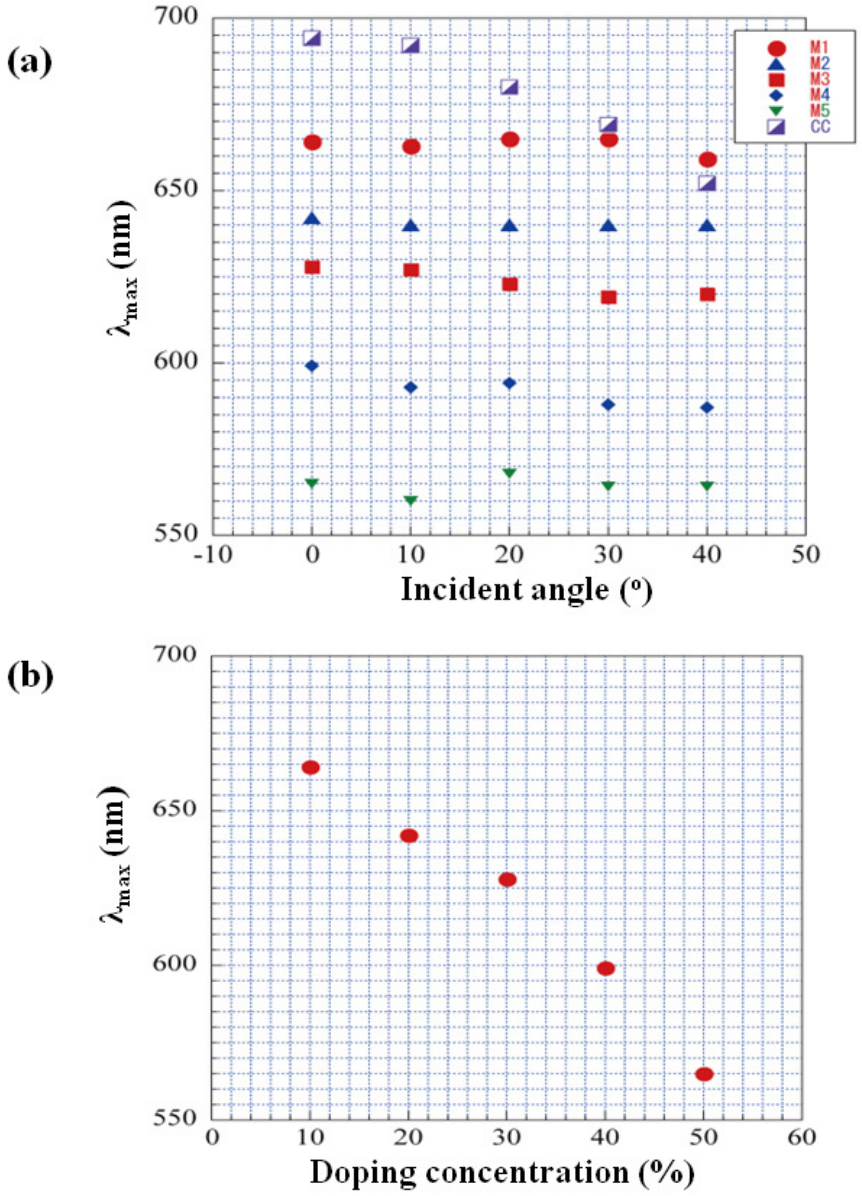

Figure 3.13. Influence of change in the angle of illumination on peak position in transmittance spectra (a) and the influence of doping concentration on peak position in transmittance spectra (b).

Due to the presence of periodic arrays with long-range and short-range order, colloidal crystals composed of submicron-sized particles are able to exhibit structural color originating from a PBG. It is believed that either periodic or quasi-periodic photonic crystals possess PBGs because these crystals have both long-range and short-range order.[6–7] The theories behind the phenomenon of the electronic band gap created in a semiconductor are commonly applied to explain the PBG in a photonic crystal. [8–9] There are some approximative models explaining the electronic band gaps in semiconductors (*e.g.*, a free electron model and a tight bonding model). The free electron model can be applied to explain PBGs in periodic structured materials, while the tight bonding model may sometimes be applied to PBGs in amorphous systems. Based on the tight binding model, we can assume that PBG can be formed in photonic amorphous materials by bonding and antibonding states of Mie resonances within each particle because they have short-range order in their structures. According to this understanding, neither lattice regularity nor long-range order is essential for the presence of a PBG in a material. It can be assumed that an amorphous structure is capable of exhibiting PBGs and thereby possessing structural color. Indeed, some theoretical results have been reported stating that PBGs can be formed in amorphous structures in spite of the complete lack of lattice periodicity.[8–10] The localization of light may be also important phenomenon to explain our results. [11] A local and spatially isotropic structural correlation, but little long-range correlation leads to strong backscattering over a relatively narrow range of optical frequencies and little variation with angle of incidence. Thus, localization of light can be generated from coherent scattering and interference. Randomness in the positions of dielectric scatterers leads to a mixing of all nearly degenerate photon branches; the complete or large photonic bad gap observed in periodic materials can be replaced by a broad

pseudo-gap consisting of localized states. [12–13] As a result, the colloidal amorphous arrays can display angle-independent structural colors due to the wavelength-selective scattering of light from the amorphous structure.

3.5. References

[1] R. Mayoral, J. Requena, J. S. Moya, C. Lopez, A. Cintas, H. Miguez, F. Meseguer, L. Vazquez, M. Holgado, A. Blanco, *Adv. Mater.* **1997**, *9*, 257-260.

[2] J. F. Bertone, P. Jiang, K. S. Hwang, D. M. Mittleman, V. L. Colvin, *Phys. Rev. Lett.* **1999**, *83*, 300-303.

[3] Y. Takeoka, T. Seki, *Langmuir* **2006**, *22*, 10223-10232.

[4] C. Paquet, M. Allard, G. Gledel, and E. Kumacheva, *J. Phys. Chem. B* **2006**, *110*, 1605-1607.

[5] E. R. Dufresne, H. Noh, V. Saranathan, S. G. J. Mochrie, H. Cao, R. O. Prum, *Soft Matter* **2009**, *5*, 1792-1795.

[6] E. Yablonovitch, *Phys. Rev. Lett.***1987**, *58*, 2059-2062.

[7] Y. Q. Wang, Y. Y. Wang, S. Feng, Z. Y. Li, *Europhys. Lett.* **2006**, *74*, 49-54.

[8] H. Miyazaki, M. Hase, H. T. Miyazaki, Y. Kurokawa, N. Shinya, *Phys. Rev. B* **2003**, *67*, 235109 (1-5).

[9] K. Edagawa, S. Kanoko, M. Notomi, *Phys. Rev. Lett.* **2008**, *100*, 013901(1-4).

[10] C. J. Jin, X. D. Meng, B. Y. Cheng, Z. L. Li, D. Z. Zhang, *Phys. Rev. B* **2001**, *63*, 195107(1-5).

[11] S. John, *Phys. Today* **1991**, 32-40.

[12] P. D. Garcia, R. Sapienza, A. Blanco, C. Lopez, *Adv. Mater.* **2007**, *19*, 2597-2602.

[13] S. John, *Phys. Rev. Lett.* **1987**, *58*, 2486-2489.

CHAPTER 4

POTENTIAL APPLICATIONS

4.1. Introduction

Recently, there has been an intensive effort to develop soft materials such as hydrogels having a periodic variation in refractive index to make way for new applications in optical devices.[1-27] Specially, the development of the stimuli-responsive chromic materials[28-31] has attracted the scientists for application in smart windows, displays and switches. Photonic crystals that are three-dimensionally periodic on a length scale comparable to the wavelength of light must be considered promising candidates for stimuli-responsive, full-color chromic materials. The color of the crystals is caused by a photonic bandgap (PBG) that forbids the propagation of electromagnetic waves in a certain frequency range.[32,33] It is technically possible to control the energy levels in the PBG by changing the periodicity and the average dielectric constant of the photonic crystals. Indeed, a close-packed colloidal crystal (CCC), which is selfassembled from monodisperse colloidal particles, offers a simple route to the fabrication of photonic crystals and can produce many desired colors. [34-37] The CCC appears to be a powerful tool for preparing stimuli-responsive chromic materials.[38-42] For the fabrication of smart materials several kinds of methods are being applied, template synthesis or the imprinting technique is one of the methods among those applied methods[43]. Structural colored gels with specific functional activity have been prepared by applying template synthesis approach [44-51]. The main parts of structural colored gels are the covalently cross-linked polymer networks and the periodically ordered structures. As a result the gel inherits physical and chemical characteristics imposed by the templates and able to recall the spatial position and three dimensional shapes of the templates due to the presence of crosslinker which is used during polymerization. But the smart materials prepared from crystalline structured template display angle dependent structural color. That means the structural

color displayed by the stimuli responsive gel changes as the direction of view (viewing angle) as well as angle of incident light (angle of illumination) change.

To devise a non-fading full color wide-angle reflective display without using color filters, the angle dependence of structural color has become a vital issue. So exhibition of angle independent or low angle dependent structural color by smart materials holds a great demand in material research. As the stimuli-responsive structural colored gel prepared from crystalline micro-structure, exhibits viewing-angle dependent structural color, so our hypothesis was to prepare stimuli-responsive porous gel which will be able to display viewing angle independent structural color by using amorphous microstructure as template. The application of the amorphous microstructure as template to fabricate stimuli-responsive angle-independent structural colored gel has been described in this chapter.

4.2. Stimuli-responsive Gel

A well-known thermo-sensitive monomer, *N*-isopropylacrylamide (NIPA)[2M], N,N'-Methylene bisacrylamide (BIS) [20mM], Azobisisobutyronitrile (AIBN) [6mM] and 1-4 Dioxane were used as the main monomer, cross-linker, initiator and solvent, respectively, to obtain stimuli-responsive gel. First, 4.5264 g of NIPA and 61.68 g of BIS were dissolved in a 20 mL of 1, 4-dioxane. The solution was degassed by bubbling nitrogen gas for 30 min before the gelation. The stable dried 3D colloidal amorphous structure was obtained by previously described method. In this case the doping concentration was 10 wt. % and the thickness was 0.6 mm. This silica–air amorphous microstructure is able to serve as mesoscopic templates for the formation of mesoporous polymer gel. The infiltrated monomer solution in the template was polymerized with AIBN as a free-radical initiator at 60 °C so as to trap

their amorphous periodical order. The obtained gels were soaked in 5% hydrofluoric acid solution for a few hours to remove the silica colloids. The resulting gels were carefully washed with pure water and allowed to reach an equilibrium swelling state in water at 25 °C. Figure 4.1 shows the fabrication of temperature sensitive porous NIPA gel, which displays viewing angle independent structural colors at different temperatures.

4.3. Structural Color Observation

The porous NIPA gel is very sensitive to the temperature change of its surroundings.[52] Depending on the change in temperature this porous gel exhibits different structural color. But the specialty of this structural color (figure 4.2) is that it is almost uniform from any viewing angle between 0^o to 40^o. Previously fabricated stimuli responsive structural colored gels [21-27, 40-52], which were prepared from colloidal crystal display viewing angle dependent structural color. So in the case where the iridescent structural color is not required, our non-iridescent structural color will be a good solution, especially in devising the smart display with a wide viewing angle.

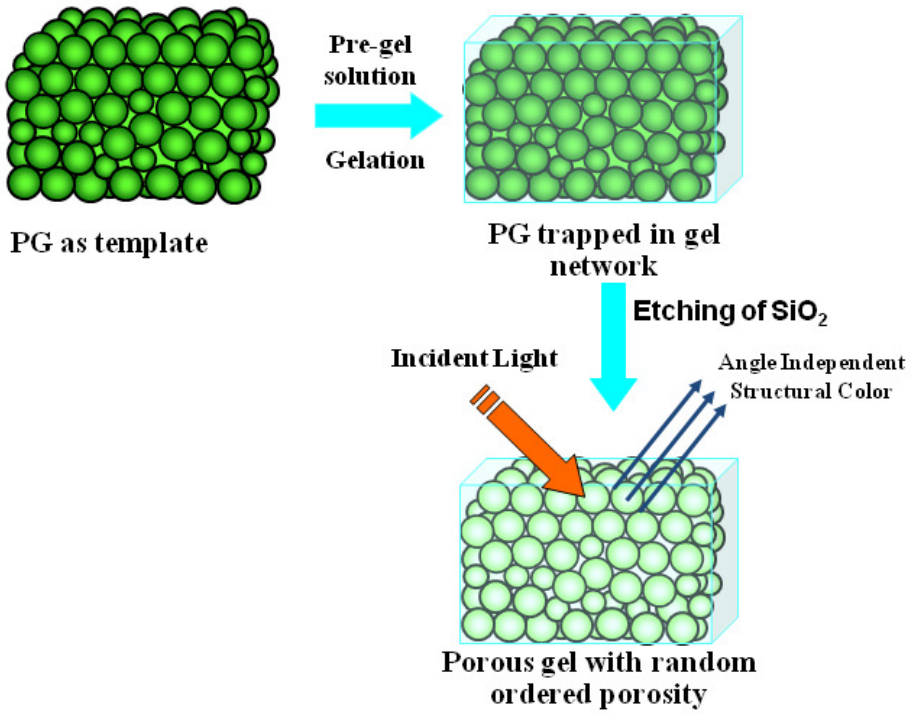

Figure 4.1. Schematic representation for the fabrication of angle-independent structural colored porous gel.

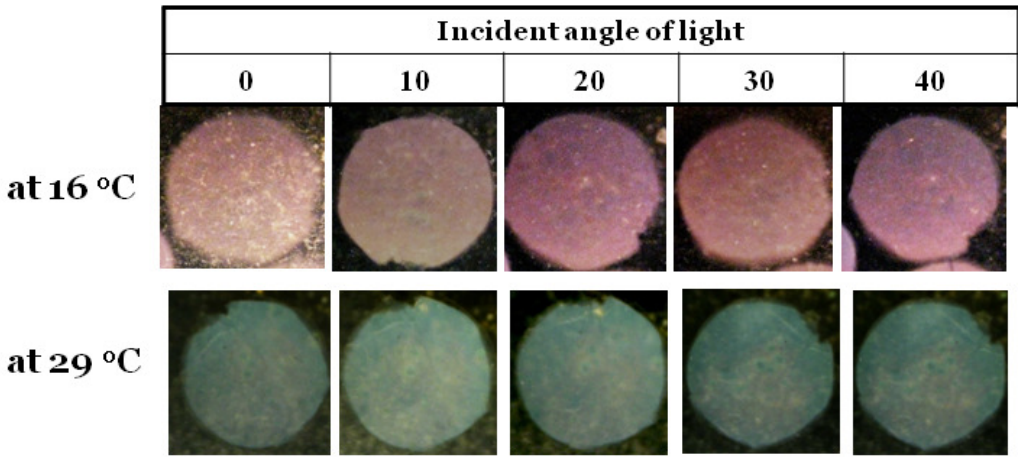

Figure 4.2. angle independent structural colors displayed by thermo-responsive porous NIPA gel at different temperature.

4.4. References

[1] Satoh, N.; Tsujii, K. *Langmuir***1992**, *8*, 581−584.

[2] Yamamoto, T.; Satoh, N.; Onda T.; Tsujii, K. *Langmuir***1996**, *12*, 3143−3150.

[3] Tsujii, K.; Hayakawa, M.; Onda, T.; Tanaka, T. *Macromolecules***1997**, *30*, 7397−7402.

[4] Weissman, J. M.; Sunkara, H. B.; Tse, A. S.; Asher, S. A. *Science***1996**, *274*, 959−960.

[5] Reese, C. E.; Mikhonin, A. V.; Kamenjicki, M.; Tikhonov, A.; Asher, S. A. *J. Am. Chem. Soc*. **2004**, *126*, 1493−1496.

[6] Holtz, J. H.; Asher, S. A. *Nature***1997**, *389*, 829−832.

[7] Liu, L.; Li, P.; Asher, S. A. *Nature***1998**, *397*, 141−144.

[8] Debord, J. D.; Lyon, L. A. *J. Phys. Chem. B***2000**, *104*, 6327−6331.

[9] Lyon, L. A.; Debord, J. D.; Debord, S. B.; Jones, C. D.; McGrath, J. G.; Serpe, M. J. *J. Phys. Chem. B***2004**, *108*, 19099−19108.

[10] Hu, Z.; Lu, X.; Gao, J. *Adv. Mater*. **2001**, *13*, 1708−1712.

[11] Lee, Y.-J.; Braun, P. V. *Adv. Mater.* **2003**, *15*, 563−566.

[12] Foulger, S. H.; Jiang, P.; Lattam, A. C.; Smith, D. W.; Ballato, J. *Langmuir***2001**, *17*, 6023−6026.

[13] Foulger, S. H.; Jiang, P.; Lattam, A. C.; Smith, D. W.; Ballato, J. Dausch, D. E.; Grego, S.; Stoner, B. R. *Adv. Mater.* **2003**, *15*, 685−689.

[14] Tsuji, S.; Kawaguchi, H. *Langmuir***2005**, *21*, 8439−8442.

[15] Fudouzi, H.; Xia, Y. *Adv. Mater.* **2003**, *15*, 892−896.

[16] Fudouzi, H.; Xia, Y. *Langmuir***2003**, *19*, 9653−9660.

[17] Arsenault, A. C.; Miguez, H.; Kitaev, V.; Ozin, G. A.; Manners, I. *Adv. Mater.* **2003**, *15*, 503−507.

[18] Fleischhaker, F.; Arsenault, A. C.; Wang, Z.; Kitaev, V.; Peiris, F. C.; Freymann, G. v.; Manners, I.; Zentel, R.; Ozin, G. A. *Adv. Mater.* **2005**, *17*, 2455–2458.

[19] Iwayama, Y.; Yamanaka, J.; Takiguchi, Y.; Takasaka, M.; Ito, K.; Shinohara, T.; Sawada, T.; Yonese, M. *Langmuir***2003**, *19*, 977–980.

[20] Yoshino, K.; Kawagishi, Y.; Ozaki, M.; Kose, A. *Jpn. J. Appl. Phys.***1999**, *38*, 786–788.

[21] Takeoka, Y.; Watanabe, M. *Langmuir***2002**, *18*, 5977–5980.

[22] Takeoka, Y.; Watanabe, M. *Langmuir***2003**, *19*, 9104–9106.

[23] Takeoka, Y.; Watanabe, M. *Langmuir***2003**, *19*, 9554–9557.

[24] Takeoka, Y.; Watanabe, M.; Yoshida, R. *J. Am. Chem. Soc*. **2003**, *125*, 13320–13321.

[25] Takeoka, Y.; Watanabe, M. *Adv. Mater.***2003**, *15*, 199–201.

[26] Nakayama, D.; Takeoka, Y.; Watanabe, M.; Kataoka, K. *Angew. Chem.***2003**, *4*, 4197–4200.

[27] Saito, H.; Takeoka, Y.; Watanabe, M. *Chem. Commun.***2003**, 2126–2127.

[28] K. Bange, T. Gambke, *Adv. Mater.* 1990, **2**, 10.

[29] D. R. Rosseinsky, R. J. Mortimer, *Adv. Mater.* 2001, **13**, 783

[30] T. Yoshioka, T. Ogata, T. Nonaka, M. Moritsugu, S.-N. Kim, S. Kurihara, *Adv. Mater.* 2005, **17**, 1226

[31] W. A. Gazotti, G. Casalbore-Miceli, A. Geri, A. Berlin, M. A. De Paoli, *Adv. Mater.* 1998, **10**, 1522.

[32] E. Yablonovitch, *Phys. Rev. Lett.* 1984, **58**, 2059.

[33] S. John, *Phys. Rev. Lett.* 1984, **58**, 2486.

[34] N. D. Denkov, O. D. Velev, P. A. Kralchevsky, I. B. Ivanov, H. Yoshimura, K. Nagayama, *Nature* 1993, **361**, 26.

[35] P. Jiang, J. F. Bertone, K. S. Hwang, V. L. Colvin, *Chem. Mater.* 1999, **11**, 2132.

[36] S. Wong, V. Kitaev, G. A. Ozin, *J. Am. Chem. Soc.* 2003, **125**, 15589.

[37] R. Mayoral, J. Requena, J. S. Moya, C. Lopez, A. Cintas, H. Miguez, F. Meseguer, L. Vazquez, M. Holgado, A. Blanco, *Adv. Mater.* 1997, **9**, 257.

[38] W. Qian, Z.-Z. Gu, A. Fujishima, O. Sato, *Langmuir* 2002, **18**, 4526.

[39] S. Kubo, Z.-Z. Gu, K. Takahashi, A. Fujishima, H. Segawa, O. Sato, *J. Am. Chem. Soc.* 2004, **126**, 8314.

[40] Y. Takeoka, M. Watanabe, R. Yoshida, *J. Am. Chem. Soc.* 2003, **125**, 13320.

[41] D. Nakayama, Y. Takeoka, M. Watanabe, K. Kataoka, *Angew. Chem. Int. Ed.* 2003, **42**, 4197.

[42] K. Matsubara, Y. Takeoka, M. Watanabe, *Angew. Chem. Int. Ed.* 2007, **46**, 1688.

[43] G. Vlatakis, L. I. Anderson, R. Muller and K. Mosbach, *Nature*, **361**, 645-647 (1993).

[44] Y. Takeoka and M. Watanabe, *Langmuir*, **18**, 5977-5980 (2002).

[45] Y. Takeoka and M. Watanabe, *Adv. Mater.*, **15**, 199-201 (2003).

[46] Y. Takeoka and M. Watanabe, *Langmuir*, **19**, 9104-9106 (2003).

[47] H. Saito, Y. Takeoka and M. Watanabe, *Chem. Commun.*, **17**, 2126-2127 (2003).

[48] D. Nakayama, Y. Takeoka, M. Watanabe and K. Kataoka, *Angew. Chem. Int. Ed.*, **42**, 4197-4200 (2003).

[49] Y. Takeoka, M. Watanabe and R. Yoshida, *J. Am. Chem. Soc.*, **125**, 13320-

13321 (2003).

[50] K. Ueno, K. Matsubara, M. Watanabe and Y. Takeoka, *Adv. Mater.*, **19**, 2807-2812 (2007).

[51] Y. Takeoka and T. Seki, *Macromolecules*, **40**, 5513-5518 (2007).

[52] Y. Takeoka and M. Watanabe, *Langmuir*, **18**, 5977-5980 (2002)

CHAPTER 5

CONCLUSIONS

5.1. Conclusions

In conclusion, we have demonstrated for the first time that solid amorphous materials prepared from silica colloidal spheres are capable of displaying angle independent structural color. Pictographic evidences along with spectrometric measurements validate that the structural color displayed by the amorphous system is independent of viewing angle and direction of incident light while the customized image analysis of scanning electron micrographs with valid theoretical explanation clarify the authentication of angle independence. More optical research for the amorphous material is needed to elucidate the exact predominant mechanism for this angle-independent structural color from the colloidal amorphous.

It is worthy to note, however, that the reported material with such optical phenomenon will be a fascinating mean to overcome technological barrier where angle dependent structural color becomes major issue for example full-color displays with wide viewing angle. Moreover this material can be used as a template to fabricate stimuli responsive structural colored soft materials and as a medium for comparative studies of optical properties with respect to colloidal crystal, to investigate light propagation in resonant amorphous system, random laser and Anderson localization.

5.2. List of Publications

Original papers

1. **Harun-Ur-Rashid, M.**, Imran, A. B., Seki, T., Ishii, M., Nakamura, H., Takeoka, Y., "*Angle-Independent Structural Color in Colloidal Amorphous Arrays*", ChemPhysChem., in press.

2. **Harun-Ur-Rashid, M.**, Imran, A. B., Seki, T., Ishii, M., Nakamura, H., Takeoka, Y.,"*Template Synthesis for Stimuli-Responsive Angle Independent Structural Colored Smart Materials* " Transactions of the Materials Research Society Japan, **34**, 333-337 **(2009).**

Review paper

Harun-Ur-Rashid, M., Seki, T., Takeoka, Y., "*Structural Colored Gels for Tunable Soft Photonic Crystals*", The Chemical Record, **9**, 87-105 **(2009)**.

5.3. Attended Conferences

1. **Mohammad Harun-ur-Rashid**, Abu Bin Imran, Takahiro Seki, Yukikazu Takeoka, Masahiko Ishii, Hiroshi Nakamura, "*Colloidal Amorphous: A Source of Viewing Angle Independent Structural Color*", FAPS polymer congress, Nagoya, **Japan**, October 20-23, 2009.

2. **Mohammad Harun-ur-Rashid**, Abu Bin Imran, Takahiro Seki, Yukikazu Takeoka, Masahiko Ishii, Hiroshi Nakamura, "*Template Synthesis of Stimuli-Responsive Angle Independent Structural Colored Gel*", Gel symposium, Tokyo, **Japan**, January 14-15, 2009.

3. **Mohammad Harun-ur-Rashid**, Abu Bin Imran, Takahiro Seki, Yukikazu Takeoka, Masahiko Ishii, Hiroshi Nakamura, "*Preparation and characterization of*

angle-independent structural colored material", 5th Yoshimasa Hirata Memorial Lecture, and The 1st G-COE International symposium on Elucidation and Design of Materials and Molecular Function, Nagoya, **Japan**, January 13-14, 2009.

4. **Mohammad Harun-ur-Rashid**, Abu Bin Imran, Takahiro Seki, Yukikazu Takeoka, Masahiko Ishii, Hiroshi Nakamura, "*Template Synthesis of Stimuli-responsive Angle Independent Structural Colored Gel*", IUMRS-ICA, Nagoya, **Japan**, December 9-13, 2008.

5. **Mohammad Harun-ur-Rashid**, Abu Bin Imran, Takahiro Seki, Yukikazu Takeoka, Masahiko Ishii, Hiroshi Nakamura, "*Template Synthesis of Stimuli-responsive Angle Independent Structural Colored Gel*", 2008 Material Research Society (MRS) Fall Meeting , Boston, MA, **U.S.A.**, December 1- 5, 2008.